

Environmental Geochemistry and Health

Geochemical characterization of the thermo-mineral waters of Greece

--Manuscript Draft--

Manuscript Number:	EGAH-D-20-00740R1
Full Title:	Geochemical characterization of the thermo-mineral waters of Greece
Article Type:	Original Research
Keywords:	Hydrogeochemistry; Stable isotopes; carbon dioxide; geothermometry
Corresponding Author:	Walter D'Alessandro Istituto Nazionale di Geofisica e Vulcanologia Palermo, ITALY
Corresponding Author Secondary Information:	
Corresponding Author's Institution:	Istituto Nazionale di Geofisica e Vulcanologia
Corresponding Author's Secondary Institution:	
First Author:	Lorenza Li Vigni
First Author Secondary Information:	
Order of Authors:	Lorenza Li Vigni Kyriaki Daskalopoulou Sergio Calabrese Konstantinos Kyriakopoulos Francesco Parello Filippo Brugnone Walter D'Alessandro
Order of Authors Secondary Information:	
Funding Information:	
Abstract:	<p>Geothermal areas of Greece are located in regions affected by recent volcanism and in continental basins characterised by elevated heat flow. Many of them are found along the coast and thus, water is often saline due to marine intrusion. In the present study, > 300 thermal and cold mineral water samples were collected along Greece. Samples were analysed for major ions, Li, SiO₂ and isotopes in water. Measured temperatures range from 6.5 to 98 °C, pH from 1.96 to 11.98, whilst Total Dissolved Solutes (TDS) from 0.22 to 51 g/L. Waters were subdivided into four main groups: i) thermal; ii) cold; iii) acidic (pH <5) and iv) hyperalkaline (pH >11). On statistical basis, the thermal waters were subdivided into subgroups according to both their temperature [warm (<29 °C), hypothermal (29-48 °C), thermal (48-75 °C) and hyperthermal (>75 °C)] and TDS [low salinity (<4 g/L), brackish (4-30 g/L) and saline (>30 g/L)]. Cold waters were subdivided basing on their pCO₂ [low (<0.05 atm), medium (0.05-0.85 atm) and high (>0.85 atm)]. δ¹⁸O-H₂O ranges from -12.7 to +2.7 ‰ vs. SMOW, while δ²H-H₂O from -91 to +12 ‰ vs. SMOW being generally comprised between the Global Meteoric Water Line and the East Mediterranean Meteoric Water Line. Positive δ¹⁸O shifts with respect to the former are mostly related to mixing with seawater, while only for a few samples they point to high-temperature water-rock interaction processes. Only a few thermal waters gave reliable geothermometric estimates, suggesting reservoir temperatures between 80 and 260 °C.</p>
Response to Reviewers:	<p>Reply to the reviewers</p> <p>Reviewer #1 The article entitled "Geochemical characterisation of the thermo-mineral waters of</p>

Greece", present comprehensive overview on the geochemical characterisation of thermomineral waters from Greece. The research article takes into consideration more than 300 original data. This is the first article on Greece where the the origin and distribution of the thermo-mineral waters are discussed using both chemical and isotopic data at the same time.

The topic is really interesting for the scientific community and the data are valuable. The article gives also helps in understanding the lack in the current research and give an insight on which Greek areas are studied in more detail. The paper is well written (for no mother tong English speaker); I could follow the thread of the discussion. In the introduction, the scientific content and state of the art are clearly written.

Some minor suggestion that could help in the better overview of the data:

1. A paragraph should be added discussing the hydrogeological settings. Even a general overview is sufficient.

Reply: We added a few sentences describing the overall hydrogeological setting of Greece.

2. In the case of the Local Meteoric Water Lines (LMWL) please insert all the available LMWL's, Or mention which were selected to be used and why. I believe for a region so big there are more than one LMWL.

Reply: The referee correctly supposes that more than one LMWL was defined for different areas in Greece. These are reported in the cited paper of Argiriou and Lyloudis, 2006. The same authors state that these LMWLs are generally not statistically different from that obtained considering all the published data on meteoric waters collected in Greece from 1960 to 2003 except for a few sites were the collected data were too few. We therefore decided to use the LMWL defined with the whole dataset which is statistically more robust. Nevertheless, we specified in the text who the LMWL was defined.

3. A ternary plot using would Cl-SO₄-HCO₃ would be useful in describing the geochemical characteristics with the geological settings of the waters.

Reply: We included the Cl-SO₄-HCO₃ ternary plot in the geothermometry section and we added an introductory/explanatory paragraph.

4. Please indicate why in the Giggenbach-diagram that one point falls above the full equilibrium line. Give possible answers for it.

Reply: We added some hypothesis.

5. For the geothermometers please add a supplementary file with the written equations.

Reply: Added

and finally 6. Add a paragraph putting into context the waters and the observed geochemical data on the gases (the published data mentioned in the text).

Reply: We added a paragraph where we talk about the relations between tectonics and fluids.

Taking into consideration the manuscript, data etc. I suggest the paper should be expected after minor revision.

Reviewer #3

Dear Authors,

In this paper (EGAH-D-20-00740) "Geochemical characterization of the thermo-mineral waters of Greece", the authors present a large dataset on the chemical and isotopic composition of the thermo-mineral waters in Greek. The topic is certainly interesting to geochemistry community and Environmental Geochemistry and Health readership

however the text does not seem an original research, as they state, but rather a synthesis of data (hyperalkaline waters dataset coincide with data from Li Vigni et al. 2020 (Ital. J. Geosci., Vol. 140, No. 1 (2021), <https://doi.org/10.3301/IJG.2020.20>, but the authors fail to mention it through the text and also in the tables). In my opinion the paper show various critical issues. First of all, the scope of the work is limited, and although the authors aim to understand the relationship between water chemistry and geological context, this goal is not pursued and discussed. The results are well presented and the subdivision of the dataset into different groups is certainly acceptable. However, within each water group there are differences in the chemical composition or variations of chemical-physical parameters that are not always justified through a geochemical approach (inter-elemental relationships, R-mode factor analysis etc). Some conclusions are obtained from previous papers and not appropriately proposed and argued on the data available. As a consequence, I think that this paper cannot be accepted for publication in the present form therefore I recommend to rewrite it and organize a new version, probably as review, and subsequently submit it again.

Reply: We acknowledge the constructive criticism of the reviewer and his/her efforts to improve the manuscript. Some very interesting points were raised and we hereby address them. The reviewer claims that "the text does not seem an original research, as they state, but rather a synthesis of data (hyperalkaline waters dataset coincide with data from Li Vigni et al. 2020 (Ital. J. Geosci., Vol. 140, No. 1 (2021), <https://doi.org/10.3301/IJG.2020.20>, but the authors fail to mention it through the text and also in the tables". All the references are included in the supplementary material Table under the name "References", while we added a phrase in the text to make it more evident. We also specified it in the abstract. Moreover, we have rewritten the scope of this work by including all the topics discussed in the manuscript in the introductory part. We consider that this addition will make the manuscript more clear. Also, we added more plots where we integrated and interpreted the data. Previous explanations were taken into consideration: Finally, we are sceptical of the reviewer's suggestion on re-submitting this article as a review. Indeed, a great number of data is discussed in the manuscript, however only one third of the dataset comprises published data; the rest is unpublished and non-peer reviewed and new concepts are introduced. Hence, we ask for the editor's opinion on the topic.

General Remarks

1) Given that the main objective of the paper is to understand the relationship between water chemistry and geological context It would be appropriate to insert a geological-structural map of Greece. The proposed geological map is not suitable as it does not show the type of outcropping rocks. The Moho depth model is not suitable for the submitted paper.

Reply: We included a map with the isopic zones of Greece in Figure 2, and deleted the map of the crustal thickness. The description of the zones, was added in the study area section.

2) in the text some places are recalled several times, can you add them in the Figure 1?

Reply: Added

3) I suggest to integrate Materials and methods section by inserting the methodology used to measure the bicarbonate in water with high pH values; In the table 1 I suggest to add Ionic Balance

Reply: Although expressed as mg of bicarbonate per litre, what we determined was total alkalinity as indicated in the text and in the supplementary table. Ionic Balance was added.

4) Cold gas-rich and Thermal waters show different Kind of hydrofacies, from CaMg-HCO₃ to NaCl. Why? Which geochemical processes can explain this?

Reply: We tried to explain the processes bringing to such great variety of hydrofacies in the discussion also adding some binary correlation plot as suggested below by the

reviewer

5) About sixteen Cold gas-rich waters have a NaCl hydrofacies. Why Only few of these waters show important seawater admixing in the dH vs. Cl binary diagram?

Reply: Most of the cold gas-rich waters pertaining to NaCl hydrofacies were originally very diluted waters so that even small admixtures of seawater changed their composition to NaCl waters.

6) When you discuss each water group it would be appropriate to report a graph that justifies the chemical composition and highlights possible differences;

Reply: We inserted binary diagrams in order to better discuss the processes acting in the hydrological circuits of the sampled waters.

7) For Cold gas-rich waters I suggest to use the Bicarbonate vs Ca+Mg and Na vs Cl diagrams in order to verify which geochemical processes take place (i.e. water-rock interaction; seawater mixing, mixing between deep and shallow water etc...)

Reply: We inserted the requested binary diagrams both for the cold gas-rich and for the thermal waters. These were discussed trying to evidence the geochemical processes taking place.

8) For thermal waters, if dissolved sulphate is due to gypsum-rich Triassic evaporates, can you verify this through graphs? Are the redox conditions suitable to the reduction of sulphate into H₂S?

Reply: Ca vs SO₄ binary diagrams were inserted and discussed. We discussed also the processes leading to the reduction of sulfates to sulfides.

9) I suggest to check the Heat flow map with waters recording the highest values of geothermometric estimations.

Reply: We evidenced the samples with the highest geothermometric estimations on the heat flow map.

10) Have you verified if any tectonic structures carry deep fluids towards the surface?

Reply: We added a paragraph where we talk about the relations between tectonics and fluids as requested also by reviewer #1.

[Click here to view linked References](#)

Geochemical characterisation of the thermo-mineral waters of Greece

5

Lorenza Li Vigni¹, Kyriaki Daskalopoulou^{2,3}, Sergio Calabrese^{1,4}, Konstantinos Kyriakopoulos⁵,
10 Francesco Parello¹, Filippo Brugnone¹, Walter D'Alessandro^{4*}

1) University of Palermo, DiSTeM, via Archirafi 36, Palermo, Italy

15 [22\) University of Potsdam, Institute of Geosciences, Karl-Liebknecht-Str. 24-25, Potsdam Golm
Germany](#)

[3\) GeoForschungs Zentrum, Physics of Earthquakes and Volcanoes, Helmholtzstraße 6/7, Potsdam,
Germany](#)

[34\) Istituto Nazionale di Geofisica e Vulcanologia, sezione di Palermo, via Ugo La Malfa 153, Italy](#)

20 [45\) National and Kapodistrian University of Athens, Faculty of Geology and Geoenvironment,
Panestimioupolis, Ano Ilissia, Greece](#)

25

30

* corresponding author: walter.dalessandro@ingv.it

Abstract

Geothermal areas of Greece are located in regions affected by recent volcanism and in continental basins characterised by elevated heat flow. Many of them are found along the coast and thus, water is often saline due to marine intrusion. In the current study, we present study, →about 300 unpublished and literature data from thermal and cold mineral ~~water samples were~~waters collected along Greece. Samples were analysed for major ions, Li, SiO₂ and isotopes in water. Measured temperatures range from 6.5 to 98°C, pH from 1.96 to 11.98, whilst Total Dissolved Solutes (TDS) from 0.22 to 51 g/L. Waters were subdivided into four main groups: i) thermal; ii) cold; iii) acidic (pH <5) and iv) hyperalkaline (pH >11). On statistical basis, the thermal waters were subdivided into subgroups according to both their temperature [warm (<29 °C), hypothermal (29-48 °C), thermal (48-75 °C) and hyperthermal (>75 °C)] and TDS [low salinity (<4 g/L), brackish (4-30 g/L) and saline (>30 g/L)]. Cold waters were subdivided basing on their pCO₂ [low (<0.05 atm), medium (0.05-0.85 atm) and high (>0.85 atm)]. δ¹⁸O-H₂O ranges from -12.7 to +2.7 ‰ vs. SMOW, while δ²H-H₂O from -91 to +12 ‰ vs. SMOW being generally comprised between the Global Meteoric Water Line and the East Mediterranean Meteoric Water Line. Positive δ¹⁸O shifts with respect to the former are mostly related to mixing with seawater, while only for a few samples they point to high-temperature water-rock interaction processes. Only a few thermal waters gave reliable geothermometric estimates, suggesting reservoir temperatures between 80 and 260 °C.

55

Keywords: hydrogeochemistry, stable isotopes, carbon dioxide, geothermometry

1. Introduction

60 In the 1960s, the National Tourism Organization (NTO 1966) estimated the number of thermo-mineral springs in Greece at more than 750, with nearly 200 of which found on the islands of the Aegean Sea. Even though about a quarter of these springs is nowadays used for balneotherapeutic purposes, archaeological evidence supports the use of some of them since prehistoric times (Fytikas et al. 1999). In classical times until the end of the Roman Empire, thermo-mineral waters were highly appreciated and many of them were mentioned by poets (Homer, Pindar, Aristophanes), 65 historians (Herodotus, Diodorus Siculus, Plutarch) and geographers (Strabo, Pausanias) (Fytikas et al. 1999). At the same time, the first theories regarding their origin were developed (Plato, Aristotle) and their medical use was emphasized (Hippocrates). It is worth mentioning that, during this period, many of the thermo-mineral springs were considered sacred and were dedicated either 70 to the Nymphs or to Asclepius, the God of Medicine. Their religious significance continued until Christian times. Then, this dedication shifted either to Virgin Mary or to Agioi Anargyroi, with the latter being saints known for offering their medical services without reward (Håland 2009). Their balneotherapeutic use declined under the Byzantine Empire and grew again under Ottoman Empire, but it was not before the end of the 20th century that other uses (heat and energy production, 75 industrial use of CO₂, etc.) were applied (Fytikas 1988). In fact, Fytikas et al. (2005) documented that in the early 70's the Institute of Mineral and Geological Exploration (IGME) used for the first time the thermal water for greenhouse heating. However, the great development in geothermal field arrived in 1981 when Greece entered the European Union, and many research projects were funded by the European Commission.

80 Greece, located in a geodynamically active area of the Eastern Mediterranean, is characterised by widespread geothermal resources closely linked to the geology of the country (Papachristou et al. 2019). Its puzzling geodynamic regime contributes to the existence of an elevated terrestrial heat flow, which results in several geothermal fields containing both low and intermediate temperature fluids (Fytikas and Kolios 1979). Areas of enhanced heat flow are located in regions affected by 85 Miocene or Quaternary volcanism and in continental basins (Fytikas and Kolios 1979). The geothermal exploration has found high-enthalpy geothermal fields in Milos and Nisyros islands, in the South Active Aegean Volcanic Arc (SAAVA), and low-medium enthalpy georesources in some Aegean islands, i.e. Chios, Lesvos and Samothraki, and in several sedimentary basins of Northern and Central Greece (Mendrinou et al. 2010). Besides, many of these fields are found along the coast 90 as well as in islands and thus, thermal waters are often brackish to saline due to marine intrusion into the coastal aquifer (Lambrakis and Kallergis 2005). In fact, according to Minissale et al. (1997), the thermal springs located in the SAAVA are affected by mixing between the local meteoric waters

and the Aegean seawater, while a marine component, sometimes evolved due to processes seated in the deep thermal reservoirs, is found also in hot waters emerging along the coast of the continental basins (Duriez et al. 2008).

95

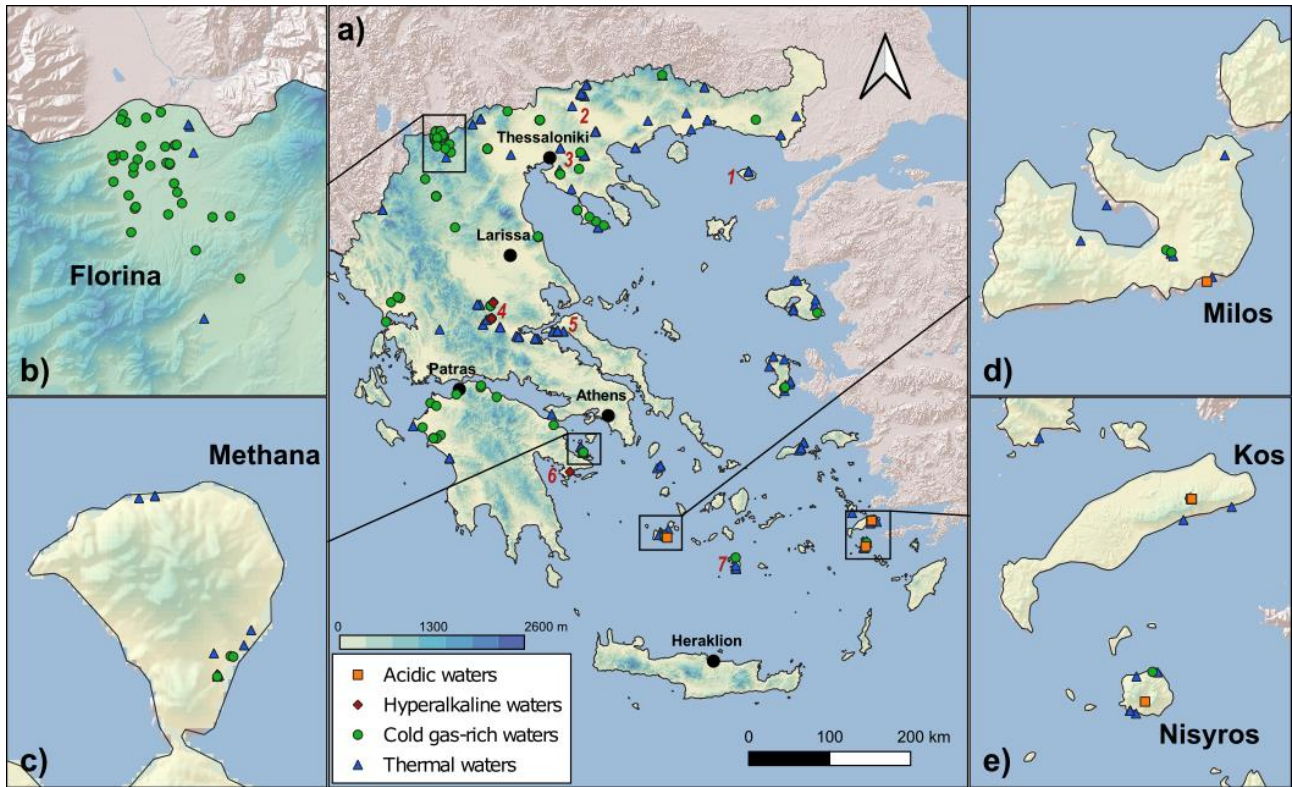


Fig. 1 – Geographic distribution of the sampling sites. Insets are enlarged areas with high density of sampling sites. 1- Samothraki; 2- Strimon Basin; 3- Migdonia Basin; 4- Othrys and Sperchios Basin; 5- Edipsos; 6 – Argolida; 7 - Santorini.

100

The complex geodynamic and geological setting of the Aegean territory reflects in a great variety of geochemical compositions for many thermal and cold fluid manifestations (Daskalopoulou et al., 2018a, 2019a, Minissale et al. 1989; 1997). The first scientific investigations regarding the chemical composition of the thermo-mineral waters of Greece appeared soon after the birth of the Modern Greek State in 1830. Landerer (1843) gave the first overview of the whole territory and further nationwide studies appeared in more recent times (Pertessis 1937; Lambrakis and Kallergis 2005; Athanasoulis et al. 2009).

105

110

The scope of this study is to present a large dataset on the chemical and isotopic composition of the thermo-mineral waters of the whole Greek country and discuss their properties in the framework of the geological context of the area. To this aim, we discussed the results of more than 300285 water samples collected from October 2004 to March 2020 (Fig.1) and analysed for their major, minor

115

and trace constituents and the isotopic composition of water. About one third of the results were previously published (D'Alessandro et al. 2008; 2011a; 2014; 2017; 2018; Li Vigni et al., 2021; Papachristou et al. 2013) and are here discussed together with the unpublished data to present a more or less complete picture of the whole country. Although spanning over a long time period, the same sampling and analytical methods were applied increasing the internal consistency of the dataset.

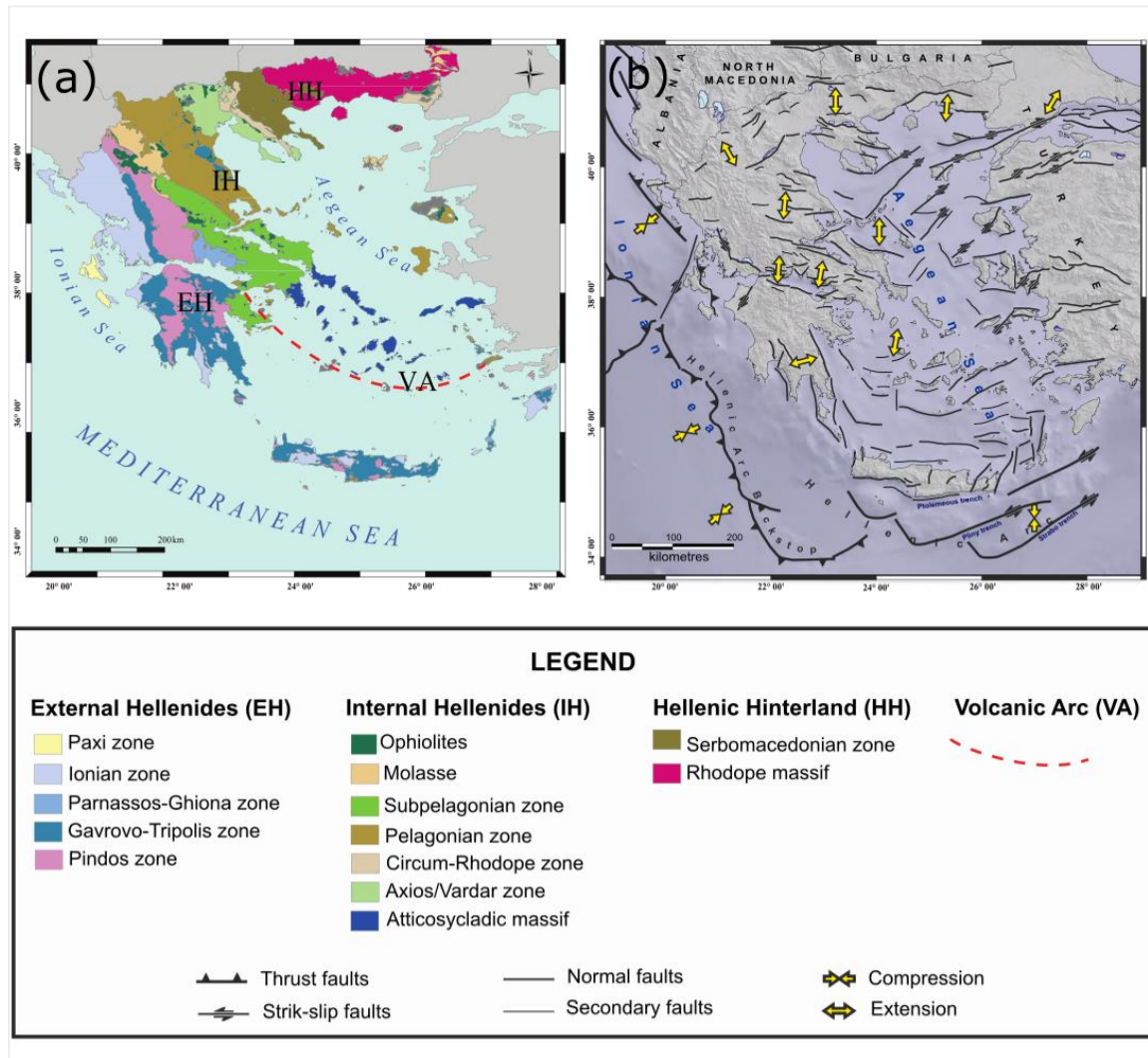
120

2. Study area

125

The complex geodynamic setting of the Hellenic territory classifies it in the most tectonically and seismically active areas of the world (e.g., Le Pichon et al. 2001; Taymaz et al. 1991; Tsokas and Hansen 1997). This regime is dominated by three large-scale tectonic structures: (i) the active retreat of the northward subduction of African plate beneath the Eurasian at a rate of 4-6 mm/a (McClusky et al. 2000) forming the back-arc Aegean area; (ii) the mostly N-S oriented crustal extension (Mercier 1981); and (iii) the westward motion of Anatolian plate along the strike-slip North Anatolian Fault (NAF) (Pavlides and Caputo 1994). It is worth noting that the Greek region is the result of the intense collision of several microplates (Aegean, Anatolian and Apulian plate) that took place during the Alpine orogenesis since the Upper Cretaceous involving the subduction of Tethyan Ocean (van Hinsbergen et al. 2005). The volcanism of the area is located in the southern Aegean Sea, while the SAAVA comprises magma of calc-alkaline to shoshonitic suite and signs of crustal contamination (Pe-Piper and Piper 2006).

130



135 Fig. 2 – Sketches illustrating the complex geodynamic situation of Greece. (a) Main geologic subdivisions (after Mountrakis, 1985): HH = Hellenic Hinterland; IH = Internal Hellenides; EH = External Hellenides; VA = Volcanic Arc; (b) Heat flow map (mW/m^2) as proposed by Fytikas and Kolios (1979); (c) The Moho depth model (km) as proposed by Grigoriadis et al. (2016); (d) map of the major tectonic structures and the current horizontal stress field main axes (Pavlides et al., 2010).

140

Based on the aforementioned complex tectonic setting and the prevailing geological formations, Mountrakis (1985, 2010) divided Greece into ~~three~~ structural isopic zones, which from west to the east are: (i)

145

(i) External Hellenides ~~that~~(EH): correspond to a neritic continental sea depositional environment; ~~(ii)~~, and consist of the Parnassos, Gavrovo-Tripolis, Ionian and Paxos zones. It is worth mentioning that during the Middle-Upper Jurassic, the Ionian zone bearded an intracontinental basin with pelagic sediments. According to Doutsos et al. (2006), three major rift structures occurred during Mesozoic within the eastern margin of the Apulian continent that were reactivated in the Tertiary by forming intracontinental thrusts;

150 (ii) Internal Hellenides, which (IH): express various environments and depending, and consist of
the Pelagonian, SubPelagonian, Atticocycladic, Circum Rhodope and Vardar zones.
Depending on the geographical position they are characterised by obducted ophiolites and
deep-sea sediments, neritic sediments, volcanoclastic and sea deposits or flysch; ~~and (iii):~~
155 ~~Hellenic Hinterland that comprises a Precambrian-Silurian continental crust affected by~~
~~metamorphism (Fig. 2a).~~ Neritic sediments prevail in the Pelagonian zone, which is
considered to be a fragment of the Cimmerian microcontinent, while obducted ophiolites are
the most characteristic lithological unit of the Subpelagonian zone. The latter is thought to be
the continental slope of the Cimmerian continent towards the ocean, whose sedimentary
remnants form the Pindos zone. Both zones consist of sea deposits, and appear a progressively
160 deepening sea towards the west. Similar to the Pelagonian, also the Attico-Cycladic zone is
envisaged as a continental fragment with undergone neritic sedimentation. Alpidic
lithostratigraphic succession bearing volcanoclastic and sea deposits ending up in deep-sea
sediments westwards, and flysch are the lithologies characterizing the Circum-Rhodope zone.
The Vardar zone corresponds to the ocean of Tethys characterized by the presence of deep-sea
165 sediments and the obducted ophiolites;

(iii) Hellenic Hinterland (HH): comprises a Precambrian-Silurian continental crust affected by
Alpidic metamorphism, and consists of the Rhodope and Serbomacedonian Massifs.
Crystalline rocks are the main lithology for both zones, while neritic deposits and Late
Eocene–Early Oligocene granitoid intrusions are present (Fig. 2a).

170 From a hydrogeological point of view, the outcropping lithologies in Greece can be subdivided in
three major groups. The first is the porous aquifers comprising mainly Quaternary and Neogene
sediments (Daskalaki and Voudouris, 2008). These are mostly found within subsident extensional
basins and cover about 30% of Greece. The second group comprises all karstic aquifers developed
both in the limestone of the sedimentary sequences and in the marble within metamorphic
175 complexes (Kallioras and Marinos, 2015). The former crop out mainly in central, western and
southern Greece and latter in the northern part of the country, altogether covering about 35% of the
whole area. The third group comprises all the remaining lithologies characterised by low
permeability or being impermeable (flysch, clays, most metamorphic rocks, volcanites, ophiolites
etc.).

180 Geology along with volcanism and tectonics favoured the existence of many thermal manifestations
and anomalous degassing areas (Daskalopoulou et al. 2019a). The elevated heat flow (Fig. 2b)
resulted in numerous geothermal fields from low to high enthalpy (Fytikas and Kolios 1979;
Andritsos et al. 2015), while the extensional tectonics (Fig. 2d2b) affected crustal thinning (Fig. 2e)

contributing to fault formation (Grigoriadis et al. 2016) and thus to the ascent of fluids. The elevated heat flow values noticed in the northern part of Greece were associated with the existence of a “first phase” volcanic arc (Fytikas et al. 1984; Vougioukalakis et al. 2004).

3. Materials and methods

The physico-chemical parameters (temperature, pH, Eh and Electric Conductivity (EC)) were measured *in situ* with portable instruments. The total alkalinity was determined by titration with 0.1 N HCl on unfiltered samples- (expressed as mgHCO₃⁻/L). Water samples were filtered (0.45 μm MF-Millipore cellulose acetate filters) and stored in HDPE bottles, whilst the aliquot for determination of cation contents was acidified with ultrapure concentrated HNO₃. Analyses of the water chemistry and the isotopic composition were carried out at the laboratories of Istituto Nazionale di Geofisica e Vulcanologia of Palermo (INGV-Pa).

Water chemistry was analysed using standard methods (APHA, AWWA, WEF, 1995): major cations (Na, K, Mg, Ca) and major anions (F, Cl, NO₃, SO₄) were determined by Ionic Chromatography (ICS-1100, Dionex), Si was determined by Inductively Coupled Plasma – Optical Emission Spectrometry (ICP-OES; Yobin Ultima). Spectrophotometric methods were used for the determination of NH₄ (Berthelot’s reaction). Lithium was determined by Inductively Coupled Plasma – Mass Spectrometry (ICP-MS; Agilent) as well as Mg and K, when found below detection limits in ionic chromatography. For all these analytical methodologies, precision was always better than ±3 %. Speciation of waters and Saturation Index (SI) of main mineral phases for each water sample and the calculation of theoretical pCO₂ for cold gas-rich samples were obtained using the aqueous speciation PHREEQC software (Parkhurst and Appelo 1999).

Ionic balance (%) was calculated with the formula:

$$\frac{\{(\sum \text{cations} + \sum \text{anions}) / [(\sum \text{cations} - \sum \text{anions}) / 2]\} \times 100}{(1)}$$

where cations are Na⁺, K⁺, Mg²⁺ and Ca²⁺ and anions Cl⁻, NO₃⁻, SO₄²⁻ and total alkalinity all expressed as meq/L.

TDS (Total Dissolved Solutes) expressed in g/L is here intended as the sum of all major anions (F⁻, Cl⁻, NO₃⁻, SO₄²⁻ and alkalinity as HCO₃⁻) and cations (Na⁺, K⁺, Mg²⁺ and Ca²⁺) plus SiO₂.

The oxygen and hydrogen isotopic compositions of waters were determined by using, respectively, Analytical Precision AP 2003 and Finnigan MAT Delta Plus IR Mass-Spectrometry on unfiltered samples. Results are expressed in delta notation (‰) respect to the international standard V-SMOW (Vienna Standard Mean Ocean Water). The uncertainties are ±0.1‰ for δ¹⁸O and ±1‰ for δ²H (±1 σ).

Geothermometric estimations were obtained for some selected samples with the software Solute Geothermometers (SolGeo) that includes 35 geothermometric equations (Verma et al. 2008).

220 4. Results

4.1 Water geochemistry

The study area from where the waters were collected is characterised by a great diversity of lithologies and geodynamic environments, which is reflected in a large variety of measured physical-chemical parameters and chemical compositions (Supplementary Material – Table S1).
225 Temperatures measured at spring outlet range from 6.5 °C to 98 °C, while pH varies from 1.96 to 11.98. It is worth noting that the great majority of the samples is delimited in pH values between 5.5 and 9, whilst only few springs show either low to very low pH (< 5) or very high pH values (> 11). TDS concentrations range from 0.22 to 51 g/L. Based on the aforementioned parameters, the sampled waters were divided into cold (< 23 °C) and thermal (> 23 °C) waters, with the former
230 being subdivided according to their pCO₂ values and the latter according to their combined temperature values and TDS concentrations (low salinity, brackish and saline). Waters characterised by either very low or very high pH were considered as extra categories. The ionic balance of the cold and thermal waters is generally within the acceptable range of ±10%. Only three samples of each of these groups exceed such limit (3.2% of the cold and 1.8% of the thermal waters). On the contrary both acid (80%) and hyperalkaline (16.7%) water show often strong imbalances. These strong imbalances are not due, as normally considered, to analytical errors. They are mostly due to the presence of less common ionic species not considered in the calculation of the ionic balance. These are OH⁻ in the case of hyperalkaline waters, H⁺, NH₄⁺, ionic species of Fe, Mn, Al, Sr, Ba in the case of acidic waters, and ionic species of S(-II) and of organic molecules in the case of reduced
235 waters. Almost all of the waters with strong imbalances here considered fall within one of these categories.
240

To better discriminate the different geochemical characteristics of the different groups, the data were plotted in a Langelier-Ludwig (1942) classification diagram (Fig. 3) and are described in detail below.

245

4.1.1 Hyperalkaline waters

The hyperalkaline waters are found in the Argolida ophiolites (Peloponnese) and the ophiolitic complex of Othrys (Central Greece). Samples of this group are characterised by very high pH values (11.17 and 11.98) and low salinity (TDS < 0.63 g/L). Temperature ranges from 17.4 to

250 27.7°C, while alkalinity is ~~expressed~~ mainly accounted by OH⁻ ions. According to Barnes et al. (1967), they can be classified as Ca-OH waters (Fig. 3a).

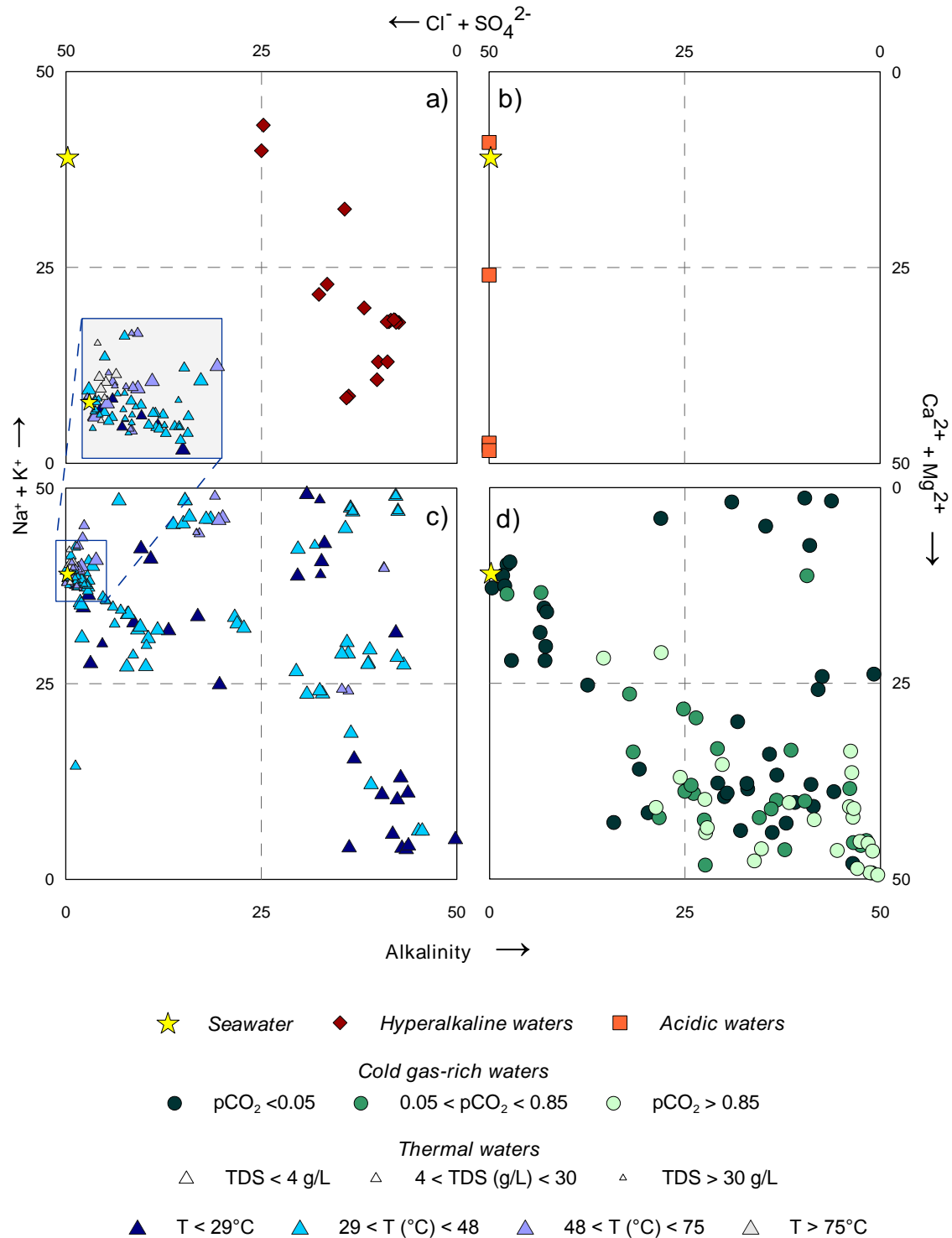


Fig. 3 – Langelier-Ludwig classification diagram for a) hyperalkaline, b) acidic, c) thermal and d) cold gas-rich waters. The yellow star represents the composition of seawater.

255

4.1.2 Acidic waters

260 The acidic waters are located in the islands of SAAVA, i.e. Kos (Kokkino Nero and Aspro Nero springs), Nisyros (Stefanos) and Milos (Paleochori). They are characterised by low pH values and a wide range of temperatures, which varies from 1.96 to 4.70 and from 13.9 to 98 °C, respectively. It should be noted that the lowest pH (1.98) and the highest temperature (98 °C) values were documented in one water sample of Stefanos crater (Nisyros). These samples are characterised by CaMg-SO₄ composition (Fig. 3b). Exception is Paleochori (Milos), which falls close to Aegean seawater point and presents the highest TDS content (51.2 g/L).

265 4.1.3 Thermal waters

Samples from this group were collected in hydrothermal fields located along the SAAVA and in continental basins. The diversity of the settings in which they were collected, results in a wide range of temperature (from 23.2 to 95.5 °C), pH (from 5.73 and 10.01) and salinity (from 0.3 to 43.2 g/L) values. Based on their temperatures and TDS content, they are subdivided into different classes (Fig. 3c); this subdivision was made following the method of Sinclair (1974) to identify statistically different populations. Three populations were detected based on TDS, while four populations were identified considering the measured temperatures (Fig. 3c). According to their water compositions, they fall into three of the quadrants of the Langelier-Ludwig diagram (Fig. 3c): (i) CaMg-HCO₃ and (ii) Na-HCO₃ water-types, which include mainly low salinity samples (< 4 g/L) and few intermediate salinity samples (4 < g/L < 30), with temperatures almost below 48 °C; (iii) NaCl composition, which includes high temperature and salinity samples with compositions that fall mostly close to the seawater point.

280 4.1.4 Cold gas-rich waters

The cold water samples are characterised by the presence of high levels of geogenic gases found in free and/or dissolved phase. Temperature ranges from 8.8 to 23 °C, pH between 5.20 and 8.72, while salinity shows a wide spectrum of values in terms of TDS (from 0.31 g/L to 30.1 g/L). Based on their CO₂ content calculated as pCO₂ using the speciation software PHREEQC (Parkhurst and Appelo 1999), they were divided into three groups; the groups were identified with the method proposed by Sinclair (1974). After plotting the samples in the Langelier-Ludwig diagram (Fig. 3d), it is noticed that the great majority of the waters with pCO₂ > 0.05 falls in the CaMg-HCO₃ field, whilst samples characterised by low pCO₂ (< 0.05) are scattered in all the sectors of the diagram.

285 4.2 Isotopic composition

290 The isotopic composition of the collected waters ranges from -12.7 to +2.7 ‰ V-SMOW for $\delta^{18}\text{O}$
and from -91 to +12 ‰ V-SMOW for $\delta^2\text{H}$. In the $\delta^2\text{H} - \delta^{18}\text{O}$ diagram (Fig. 4), the majority of the
waters fall between the Global Meteoric Water Line (Craig 1961: GMWL $\delta^2\text{H} = 8 \times \delta^{18}\text{O} + 10$) and
the East Mediterranean Meteoric Water Line (Gat and Carmi 1971: EMMWL $\delta^2\text{H} = 8 \times \delta^{18}\text{O} + 22$).
295 A Local Meteoric Water Line defined by Argiriou and Lykoudis (2006) (LMWL $\delta^2\text{H} = 7.24 \times \delta^{18}\text{O}$
 $+ 8.2$) has been also plotted. Such LMWL has been obtained by the authors including all published
isotope data on rainwater collected in Greece in the period from 1960 to 2003 (Argiriou and
Lykoudis 2006). Hyperalkaline (Fig. 4a) and most of the thermal and cold waters (Figs. 4c, 4d)
follow the Local Meteoric Water Line of Greece ~~defined by Argiriou and Lykoudis (2006) ($\delta^2\text{H} =$
 $7.24 \times \delta^{18}\text{O} + 8.2$) suggesting. This suggests~~ that the water samples have a meteoric origin, whereas
300 acidic waters show a negative shift for $\delta^{18}\text{O}$ (Fig. 4b).

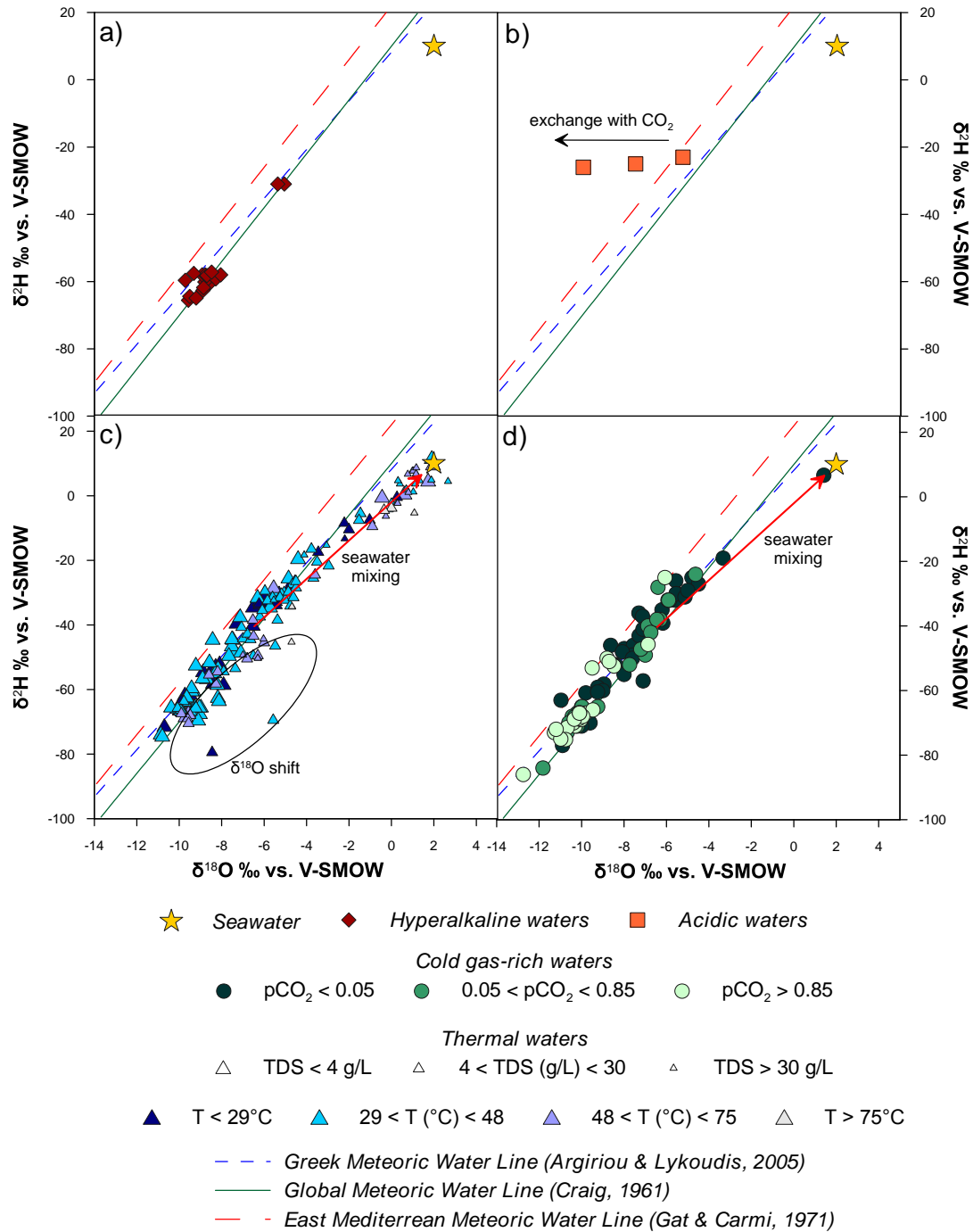
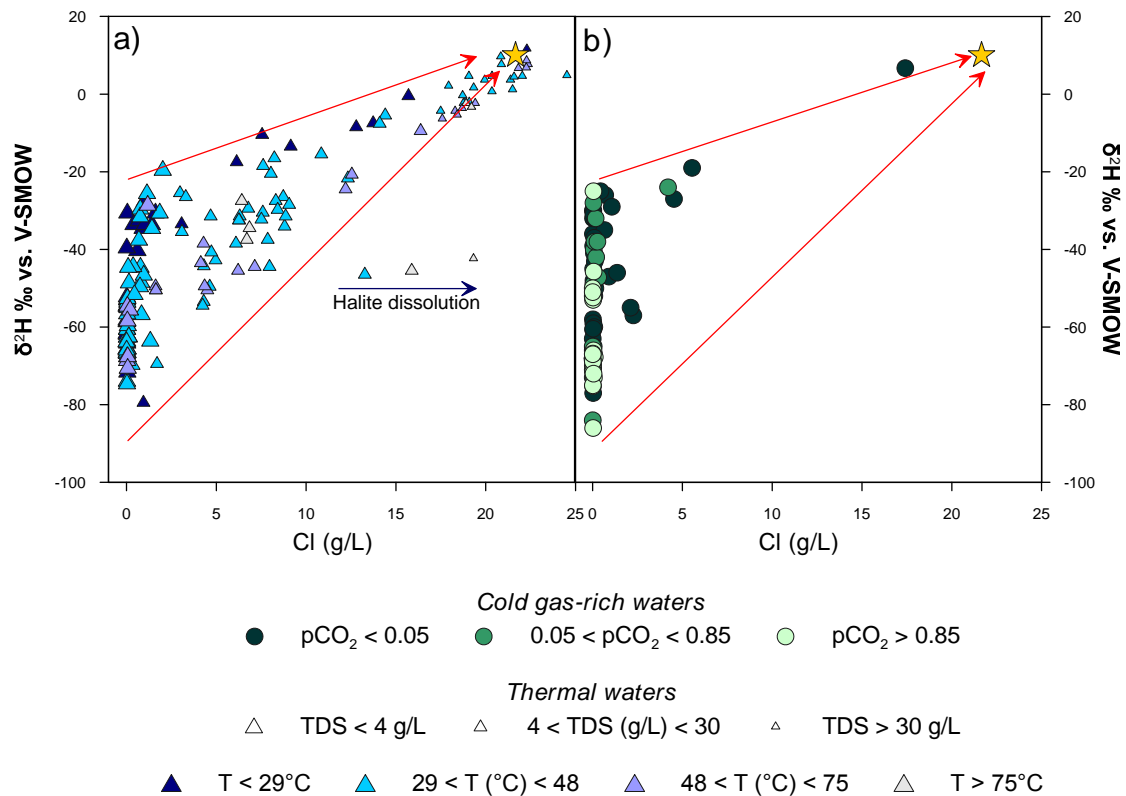


Fig. 4 – $\delta^2\text{H}$ vs. $\delta^{18}\text{O}$ binary diagrams for the sampled waters.

Some thermal and cold waters are aligned with Aegean seawater point (Figs. 4c, 4d), indicating a
 305 mixing between the meteoric water and seawater. As marked in Figs. 4c and 4d, many water
 samples show a positive $\delta^{18}\text{O}$ shift. In the case of thermal waters could indicate isotope exchange
 due to water-rock interaction at higher temperatures (Clayton and O'Neil 1972), while in the case of
 cold waters may be justified by evaporation processes.

The effect of seawater contamination can be observed in the $\delta^2\text{H}$ vs. Cl binary diagram (Fig. 5).
 310 Only few cold gas-rich waters show important seawater admixing (Fig. 5b), while this process is very widespread for the thermal waters (Fig. 5a). Some waters collected in Samothraki Island fall outside the rainwater-seawater mixing lines. For these, dissolution of Halite in Miocene evaporites have been invoked (Dotsika 2012).



315 Fig. 5 - $\delta^2\text{H}$ vs. Chloride binary diagrams for the sampled waters. Red arrows show mixing lines between the highest and lowest average isotopic value of rainwater measured in Greece (Argiriou and Lykoudis, 2006).

5. Discussion

5.1 Hyperalkaline waters

320 The ophiolitic sequences comprise widespread products derived from the hydration of ultramafic rocks, in which olivines and pyroxenes are altered to serpentine-group minerals (Evans et al. 2013). Typical features of waters circulating in serpentinized ultrabasic rocks are elevated pH values (>10), Ca-OH composition with very low concentrations of Mg^{2+} and total dissolved carbon (TDC) mainly present as CO_3^{2-} (Bruni et al. 2002). According to Barnes et al. (1967), two types of waters can be
 325 recognised in aquifers hosted in ophiolitic rocks: (i) MgCaHCO_3 waters with pH generally < 10 and (ii) hyperalkaline Ca-OH waters. The former represents the early stage of interaction between the ophiolites and meteoric waters into shallow aquifers (Cipolli et al. 2004), whilst the latter represent its evolution in deep serpentinized ultramafic aquifers under reducing environment (Bruni et al.

2002). Samples of Argolida ophiolites (Peloponnese) are represented by the Agioi Anargyroi
330 Springs, which are characterised by enhanced pH values (up to 11.98) and Ca-OH composition
(D'Alessandro et al. 2018). On the other hand, samples of Othrys (Central Greece) are characterised
by many hyperalkaline springs (pH > 11; Ekkara and Archani), which are classified as Ca-OH type
waters (D'Alessandro et al. 2014; Li Vigni et al. ~~2020~~2021).

335 **5.2 Acidic waters**

Samples of this group present characteristics similar to acidic waters as described in Giggenbach
(1988). These waters can be distinguished in three different subgroups each one belonging to a
different island of the SAAVA.

Samples collected at Kos Island are characterised by acid sulfate composition, likely related to the
340 addition of CO₂ and H₂S rich hydrothermal gases to groundwater (Giggenbach 1988), and exhibit
high concentrations of Ca²⁺ (up to 508 mg/L) and SO₄²⁻ (up to 2,774 mg/L). These springs are
found within an area of strong geogenic soil degassing (Daskalopoulou et al. 2019b). The abundant
deep hydrothermal H₂S gas dissolves in the shallow aquifer and is converted into H₂SO₄ by
oxidation with atmospheric oxygen dissolved in the meteoric recharge (Nordstrom et al. 2009).
345 Such process increases the sulfate content and lowers the pH of the water. The isotopic composition
shows a negative shift of δ¹⁸O (up to about 5 ‰ units) respect to the local meteoric water line (Fig.
4b). The effect can be the result of isotope exchange with CO₂ (Karolytè et al. 2017) at low
temperature favoured by the high gas/water ratio.

The sample of Stefanos crater (Nisyros) is characterised by an elevated temperature (98 °C), very
350 low pH value (1.98), and an acidic sulfate composition. It was collected in a boiling pool of the
hydrothermal explosion crater of Stefanos within the Lakki caldera. The crater is characterised by
strong fumarolic activity (Marini and Fiebig 2005), mainly concentrated along the rim. An area of
about 1000 m² with many tens of boiling pools is present in the middle of the crater, the water of
which probably results from the mixing of condensing fumarolic vapour and meteoric-derived
355 shallow groundwater. In the summer dry period the pools' level falls to about 1 m depth, while in
winter, after heavy rainfall, the entire bottom of the crater can be covered by rainwater, forming an
ephemeral lake. The collected sample has the typical steam heated water composition (Nordstrom et
al. 2009) with high concentrations of SO₄²⁻, low pH and high temperature. Sulfate is almost the only
anion balanced by a lot of cations including Fe, Al and NH₄⁺ that have concentrations comparable
360 to the major cations.

The Paleochori sample was collected at a small cave on the western end of Paleochori Beach
(Milos), and is characterised by high temperature (75°C) and NaCl water type. The water of the

spring comes out with gas bubbles from rocky debris and gets mixed with seawater, when the sea is rough. Its chemical composition is similar to marine water, indicating that, even if the sea is calm, contamination by seawater occurs within the shallowest part of the hydrological circuit. The area is characterised by widespread degassing both onshore as diffuse degassing from the beach and underwater as bubbling hot water (up to 120°C) springs (Daskalopoulou et al. 2018b).

5.3 Cold gas-rich waters

As mentioned in Par. 4.3, cold mineral waters have been subdivided into three statistically different populations based on their $p\text{CO}_2$ (<0.05 – from 0.05 to 0.85 and >0.85 atm), with the lowest value almost corresponding to the highest limit of organic derived soil CO_2 contribution to groundwater (Chiodini et al. 1995). Therefore, values above this limit indicate a geogenic CO_2 contribution. Recent studies (Daskalopoulou et al. 2018a; 2019a) evidenced that Greece, being a geodynamically active region, is a territory of extensive geogenic degassing. Most of the degassing activity in Greece is associated to thermal anomalies of variable intensity, but especially in Northern Greece the two phenomena are sometimes unrelated. In this area, several cold CO_2 -rich mineral waters are known and many of them are appreciated as natural soda waters suitable for human consumption, with some of them being distributed in the whole country (i.e. Doumbia, Souroti and Xino Nero). Most of the CO_2 -rich groundwater samples were collected in Florina Basin. This is one of the intramontane basins within the Hellenide Orogen, formed by the extensional tectonic regime of the area starting from the Late Miocene (Pavlidis and Mountrakis, 1987). The thick and impermeable sedimentary sequence of Florina basin favoured the existence of many CO_2 reservoirs (Karakatsanis et al. 2007). Some of these are industrially exploited by the Air Liquide Greece Company for production of dry ice and filling of pressurised gas bottles. The estimated industrial CO_2 extraction is $\sim 30,000$ t/a (Pearce et al. 2004). However, these reservoirs are leaky, thus CO_2 rises up, mainly through faults, reaching directly the atmosphere or being dissolved in great quantities in the shallow unconfined aquifers. The water extracted from many of the shallow wells (<100 m) dug or drilled in these aquifers separates a free gas phase due to the high concentration in CO_2 (D'Alessandro et al. 2011).

The equilibrium of carbonate species is regulated mainly by sources and sinks within the hydrologic circuit. The main sources are the deep-derived geogenic CO_2 dissolution and/or the dissolution of carbonate rock of the aquifers. Losses depend mainly on CO_2 exsolution due to the separation of a free gas phase as water pressure within the aquifer decreases in the shallower levels and/or on precipitation of carbonate minerals due to oversaturation. The majority of samples with high $p\text{CO}_2$

are characterised by Ca-HCO₃ composition. The dissolution of CO₂ strongly dominates the chemical evolution of the waters increasing their aggressiveness with respect to the aquifer's rocks.

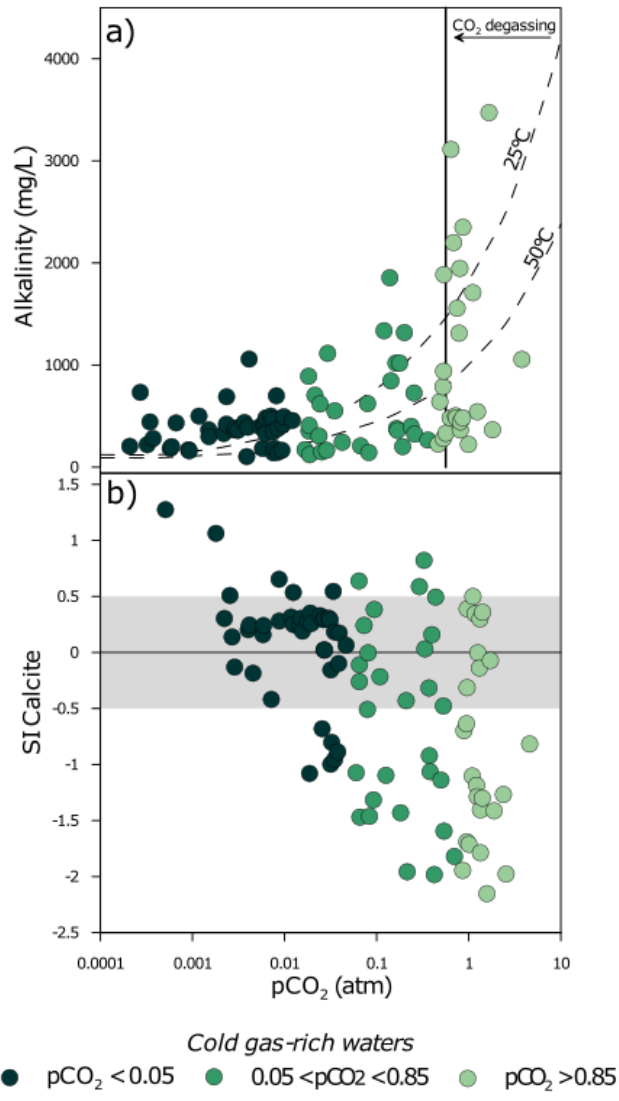


Fig. 6 – CO₂ partial pressure vs. alkalinity (a) and vs. Calcite Saturation Index (b) of the cold gas-rich waters. Dashed lines in (a) are concentrations of alkalinity (expressed as mg/L of HCO₃⁻) at the given CO₂ partial pressure at 25 and 50 °C. The grey shaded area in (b) comprises values (±0.5) considered at saturation for the given solid phase.

As a consequence, bicarbonate represents generally more than 70% by weight of their TDS and pH is slightly acidic (5.2 - 6.9). Due to the high pCO₂ values (Fig. 6a), in this group of waters, saturation or oversaturation in carbonate minerals (Calcite, Aragonite or Dolomite) is rarely achieved (Fig. 6b). In the intermediate pCO₂ population only few samples result oversaturated (Fig. 6b). Equilibrium with carbonate minerals is rarely attained in the waters with pCO₂ > 0.05 atm indicating that carbonate dissolution in these waters is not so important as the CO₂ dissolution. On the contrary, many of the waters with pCO₂ < 0.05 atm are close to equilibrium with the main carbonate minerals. These waters are from sedimentary areas, where the presence of carbonate

rocks in their aquifers is ascertained or probable and these rocks control the equilibrium of the dissolved carbonate species. In these waters the dissolved and/or, if present, the free gas phases are dominated by CH₄ or N₂ (Daskalopoulou et al. 2018a; 2019a). Geographically, these waters are mainly distributed in the western part of Greece, where CO₂ degassing is trivial and hydrocarbon-rich areas are present (Daskalopoulou et al. 2018a; 2019a).

Only few cold water samples have a NaCl composition, indicating a significant seawater contamination of the aquifers. These are located along the coastlines of continental Greece or on islands. Despite their moderately low temperatures (19.4 – 20.7°C) that classify them cold, they have been used in the past as spas and are therefore included in the present inventory. In the Na vs. Cl binary diagram (Fig. 7a) they fall along the seawater mixing line. Almost all of the low salinity waters are enriched in Na with respect to the Na/Cl ratio in seawater due to water-rock interaction processes within their aquifers.

Very few water samples plot along the 1/1 ratio line in the Ca²⁺ vs. SO₄²⁻ binary plot (Fig. 7b) suggesting only a sporadic influence of Ca-sulfate minerals dissolution. Most of the waters are strongly enriched in Ca²⁺ confirming the strong influence of Ca-carbonate dissolution. But as we will see for the thermal waters, Ca²⁺ enrichment may occur also in the case of Ca-sulfate minerals dissolution, when the thermodynamic conditions are favourable to sulfate reduction to sulfide. This is probably the case of most waters collected in the western part of Greece where Triassic evaporitic gypsum is often found in the sedimentary sequences of the area (Rigakis and Karakitsios 1998). Thermochemical sulfate reduction can be sustained by the presence of hydrocarbons in the same area (Palacas et al. 1986), which promote the sulfide formation (Machel 2001).

Most of the cold water samples are more or less aligned along the 1/1 ratio in a Ca²⁺ + Mg²⁺ vs. alkalinity binary diagram (Fig. 7c) indicating a strong influence of the congruent dissolution of carbonate minerals within their aquifers. Only in few cases the mixing of seawater can be invoked to explain a Ca²⁺ + Mg²⁺ excess with respect to the 1/1 ratio line. On the contrary most of the deviations from this line may be due to oversaturation of some carbonate species. In this case the precipitation of a solid phase will virtually enrich either the cations (Ca²⁺ and Mg²⁺) or the anion (HCO₃⁻) depending on which one is in excess with respect to the 1/1 equivalent ratio. Calcium excess may be favoured by the presence and dissolution of Ca-sulfate minerals while bicarbonate excess may derive from the dissolution of abundant geogenic CO₂. The latter process may justify the formation of the alkaline-bicarbonate waters (Fig. 3d).

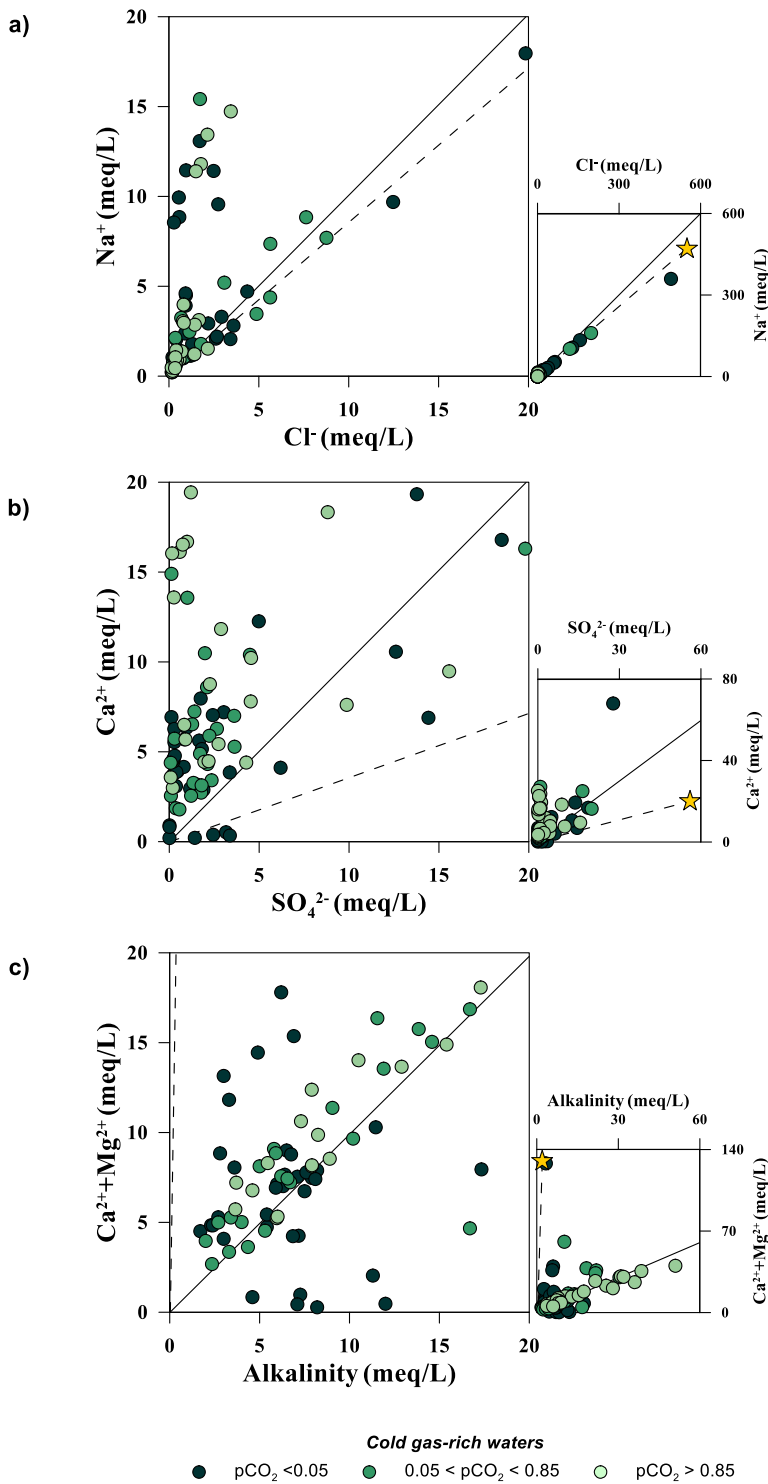


Fig. 7 – Binary correlation plots for the cold gas-rich waters. (a) Na^+ vs. Cl^- ; (b) Ca^{2+} vs. SO_4^{2-} ; (c) $\text{Ca}^{2+} + \text{Mg}^{2+}$ vs. Alkalinity. Dashed line seawater mixing line, continuous line 1/1 ratio.

445

5.4 Thermal waters

Geologically young regions like the Alpine orogen show a high variability in heat flow with respect to older cratonic areas (Pollack et al. 1993). Greece, which belongs to the Alpine orogen, makes no exception—and in the preliminary map of Fytikas and Kolios (1979), heat flow shows values that

450

range from < 30 to > 120 mW/m² (Fig. [2b10b](#)). Values above ~~65 mW/m²~~, the average continental heat flow ([65 mW/m²](#)- Pollack et al., 1993), are considered as positive anomalies. Looking at the map of Fytikas and Kolios (1979), these anomalous values are mainly found in areas with active or recent (< 10 Ma) intrusive or effusive magmatism (Pe-Piper and Piper 2002). These areas are also those with the thinnest crust (Grigoriadis et al. 2016) and subject to active extensional tectonics (Pavlidis et al. 2010 (Fig. [2e2b](#)). The highest heat flow anomalies are recorded along the SAAVA. Signs of the increased heat flow are thermal springs and thermal groundwater tapped by drillings. Therefore, it is not a surprise to find the hottest thermal waters in the areas of increased heat flow (Fig. [2b10b](#)). These thermal waters, together with fumaroles and steaming grounds, are the surface expressions of active geothermal systems. Geothermal exploration proved that two of them, located in the active volcanic systems of Milos and Nisyros, are two-phase high enthalpy fields suitable for electricity production. Explorative drillings tapped geothermal fluids with temperatures up to 320 and 340 °C respectively (Liakopoulos et al. 1991; Chiodini et al. 1993). Geothermal energy was exploited for a period by a power plant at Milos until it was stopped by the protests of the inhabitants complaining for the H₂S released by the extracted geothermal fluids (D'Alessandro et al. 2009). The remaining explored geothermal reservoirs can be defined as hot-water systems (Kaya et al. 2011).

Many of the geothermal systems are found on islands or are on the coast of continental Greece (Fig. 1). Therefore, seawater plays a major role in determining the composition of the waters released by these systems. This can be evidenced both in their chemical composition with Na/Cl ratios very close to that of seawater (Fig. [38a](#)) and in their isotopic composition (Figs. 4 and 5) nicely evidencing a mixing between meteoric and sea water. From these diagrams it cannot be deduced if seawater acts as a contaminant in the shallowest part of the hydrologic circuit or if it represents a main feeder of the geothermal reservoir. For the high enthalpy systems of Milos and Nisyros, a strong contribution of seawater to the reservoir has been ascertained from the analyses of the fluids sampled from the explorative boreholes (Liakopoulos et al. 1991; Chiodini et al. 1993). However, a clue of a seawater contribution in several other reservoirs is the fact that many of the samples plotting close to the seawater point are those with the highest temperatures (Figs. 3, 4 and 5). As we will see in par. 5.4.1, these are often waters falling in the field of the partially equilibrated waters in the Giggenbach triangular plot (Fig. [79b](#)).

Many water samples show a very high Na/Cl ratio (Fig. 8a). Almost all come from three graben areas filled by postorogenic sediments mainly deriving from the dismantling of the metamorphic rocks bordering these grabens. These are the Sperchios, Strimon and Migdonia basins. The faults bordering the grabens favoured the formation of hydrothermal systems while the ubiquitous

485 presence of Na-rich minerals (e.g. albite) in the metamorphic rocks and in the sediments from them
derived allowed the formation of Na-rich waters (Meyback 1987). For the same reasons, similar
conclusions may be drawn also for the cold gas-rich waters collected in the Florina basin and some
artesian wells along the northern and western coast of Peloponnese (Fig. 7a).

490 As seen before for the cold waters, also in the case of thermal waters very few samples fall along
the line representative of the dissolution of Ca-sulfate minerals (Fig. 8b). The great majority of the
waters are enriched in Ca²⁺ that is mostly explainable by the release of this cation by high
temperature water-rock interaction processes. But the sulfate deficit may be, at least partially,
explained by the reduction to sulphur and sulfide. While in the high temperature systems such
reduction involves only inorganic reactions in the case of lower temperatures microbiological
495 mediated sulphur reduction is also involved, sometimes presupposing the presence of thermophile
microorganisms (Chiodini et al. 1998; Brombach et al. 2003; Gilhooly et al. 2014). The rapidly
changing physico-chemical conditions in the shallowest part of the hydrothermal circuit induces
rapid changes in the oxidation state of sulfur further complicating the picture in a complex
interaction between biotic and abiotic influences on the sulfur cycle (Marini et al. 2002; Gilhooly et
500 al. 2014). This may effects also on other dissolved species like for example methane. Strong isotope
fractionation of this gas has been, in fact, attributed to anaerobic methane oxidation involving the
microbial reduction of sulfate as electron donor (Daskalopoulou et al. 2018a).

Spas in western Greece are fed by hypothermal or even cold springs. They are generally heated for
balneotherapy and considered healthy mainly for their mineral content. Most of them are rich in
505 dissolved sulfide and the exsolved H₂S can be distinctly smelled. This region corresponds to the
thick organic-rich sedimentary sequences of the External Hellenides (Fig. 2a), which are considered
the most favourable areas in Greece for hydrocarbon generation (Palacas et al., 1986; Rigakis and
Karakitsios, 1998). Thus, in the sampled waters methane is generally the dominant gas both in the
dissolved and the free gas phase (Daskalopoulou et al., 2018a; 2019a). This is the Greek region with
510 the greatest crustal thickness unfavourable to the uprise of gases and heat from the mantle ~~(Fig. 2e).~~
Therefore, this area is not prone to the formation of geothermal systems and the slight
thermalisation of the waters is mostly the consequence of the deep circulation within regional fault
systems. The stratigraphic sequences of the External Hellenides comprise often gypsum-rich
Triassic evaporites (Rigakis and Karakitsios, 1998). The presence of sulfates and hydrocarbons
515 favours the formation of H₂S through either Microbial (MSR) or Thermochemical (TSR) Sulfate
Reduction (Machel, 2001). The presence of H₂S in the water samples in western Greece is mainly
related to these processes rather than being produced in active geothermal systems.

Finally, the $\text{Ca}^{2+} + \text{Mg}^{2+}$ vs. alkalinity binary diagram (Fig. 8c) shows that the interaction with carbonate minerals is negligible and evidences two main processes affecting these waters: mixing with seawater and dissolution of geogenic CO_2 .

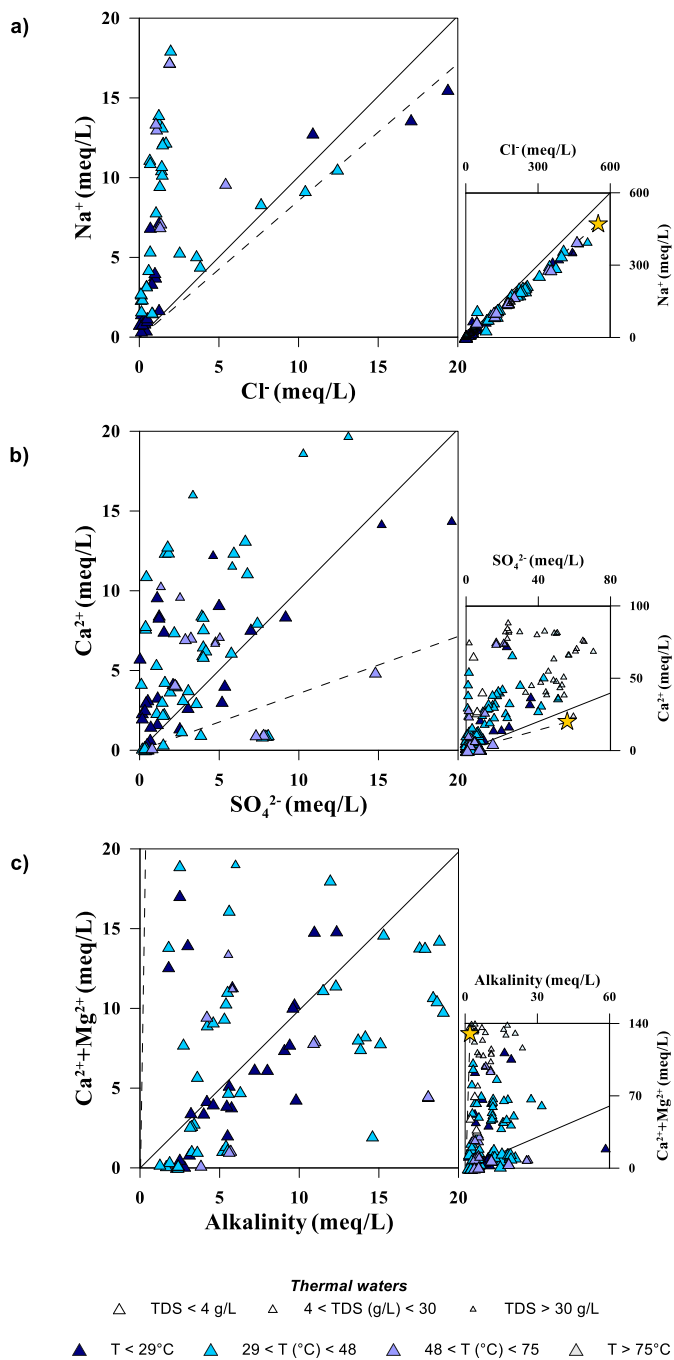


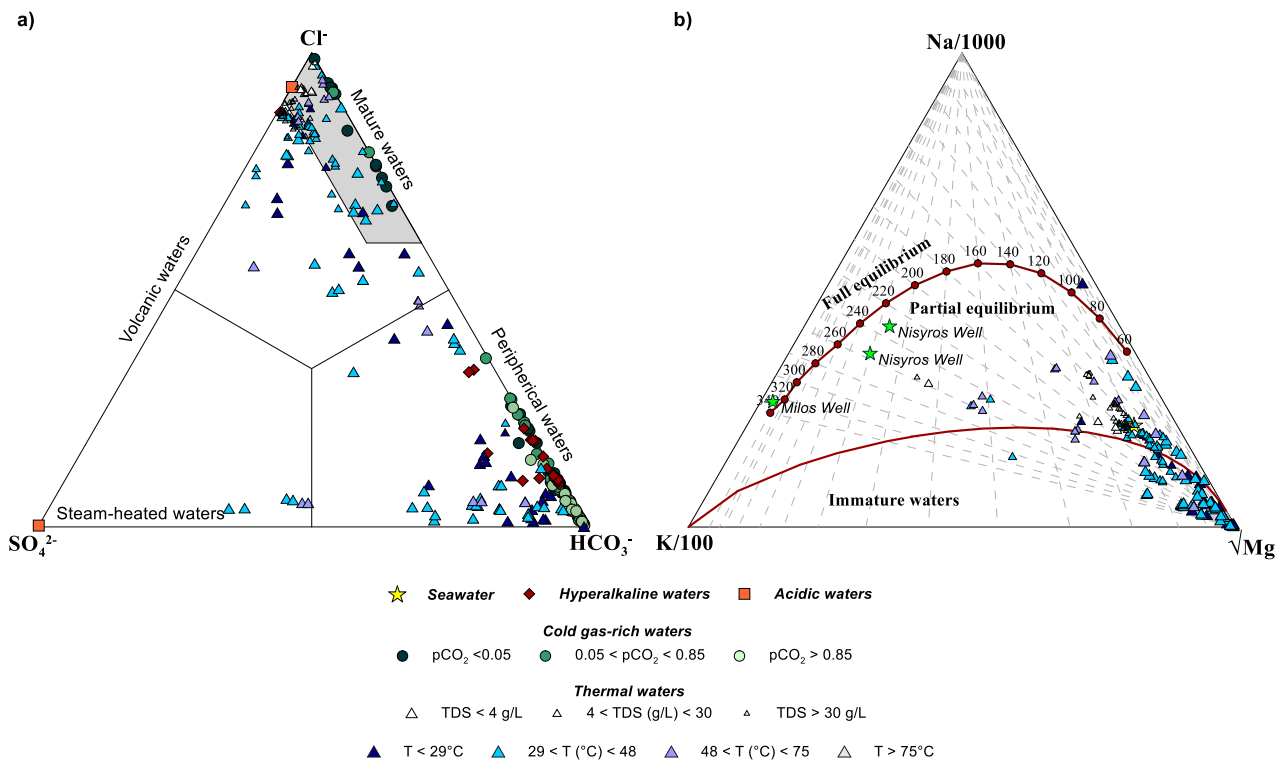
Fig. 8 – Binary correlation plots for the thermal waters. (a) Na^+ vs. Cl^- ; (b) Ca^{2+} vs. SO_4^{2-} ; (c) $\text{Ca}^{2+} + \text{Mg}^{2+}$ vs. Alkalinity. Dashed line seawater mixing line, continuous line 1/1 ratio.

5.4.1. Geothermometry

530 The ternary diagram Cl-SO₄-HCO₃ (Giggenbach, 1991) is used to examine the maturity of waters. Specifically, mature waters are characterised by high Cl content that originates from a deep-hot geothermal system, while SO₄ type waters usually derive from steam-heated water influenced either
by volcanic steam bearing high-temperature HCl or by geothermal steam bearing low-temperature H₂S (Dolgorjav 2009; Rezaei et al., 2018). On the other hand, alkaline waters are typically related to samples of meteoric origin. In the Hellenic territory, hyperalkaline waters, as well as the great majority of cold waters and some thermal waters fall in the HCO₃ field, indicating processes of mixing with the near-surface groundwater during their ascent to the surface (Singh et al., 2015)
535 (Fig. 9a). Enrichment in SO₄ is present in some thermal (Nymfopetra, Nea Apolonia (1,3,4)) waters. These samples (thermal) present low Cl content, high Na concentration and are characterised by calcite precipitation indicated by the presence of travertines in these areas. The fumarolic samples of Stefanos and Paleochori are plot in the SO₄-Cl axis, which is typical of volcanic waters, highlighting the impact of the volcanic activity on the samples. Many thermal gases fall in the field
540 of mature waters. These samples may be considered as samples not affected by secondary processes during the ascent of water to the surface that mainly derive from the deep and hot geothermal systems.

In order to evaluate the applicability of conventional geothermometric estimates, the chemical composition of the thermal waters ~~were~~was plotted on a cationic ternary diagram (Giggenbach, 545 1988) (Fig. 79b). The majority of the samples fall in the immature waters field and therefore, they have to be considered unsuitable for geothermometric estimations. Much fewer samples plot in the partial equilibrium field, while only one sample (Amplas 2) falls above the full equilibrium line. The latter refers to water in which an abundant CH₄-rich gas phase was bubbling (Li Vigni et al., 2021). Waters interacting with CH₄ are often characterised by a strong Mg depletion either because
550 they are mixed with oil field brines (Kharaka and Mariner, 1989) or with hyperalkaline water (Bruni et al., 2002; Cipolli et al., 2004).

The only samples that plot on or very close to the full equilibrium line are those taken from geothermal exploration wells at Milos (well M2 – Koutroupis, 1992) and Nisyros (well N₂ – Koutroupis, 1992; Chiodini et al., 1993). The estimated temperatures nearly correspond to that
555 measured at Milos (318 °C – Liakopoulos et al., 1991) or is not so far from that measured at Nisyros (290 °C – Chiodini et al., 1993). In the latter case Chiodini et al. (1993) hypothesize a contamination by the seawater used to prepare the drilling mud.

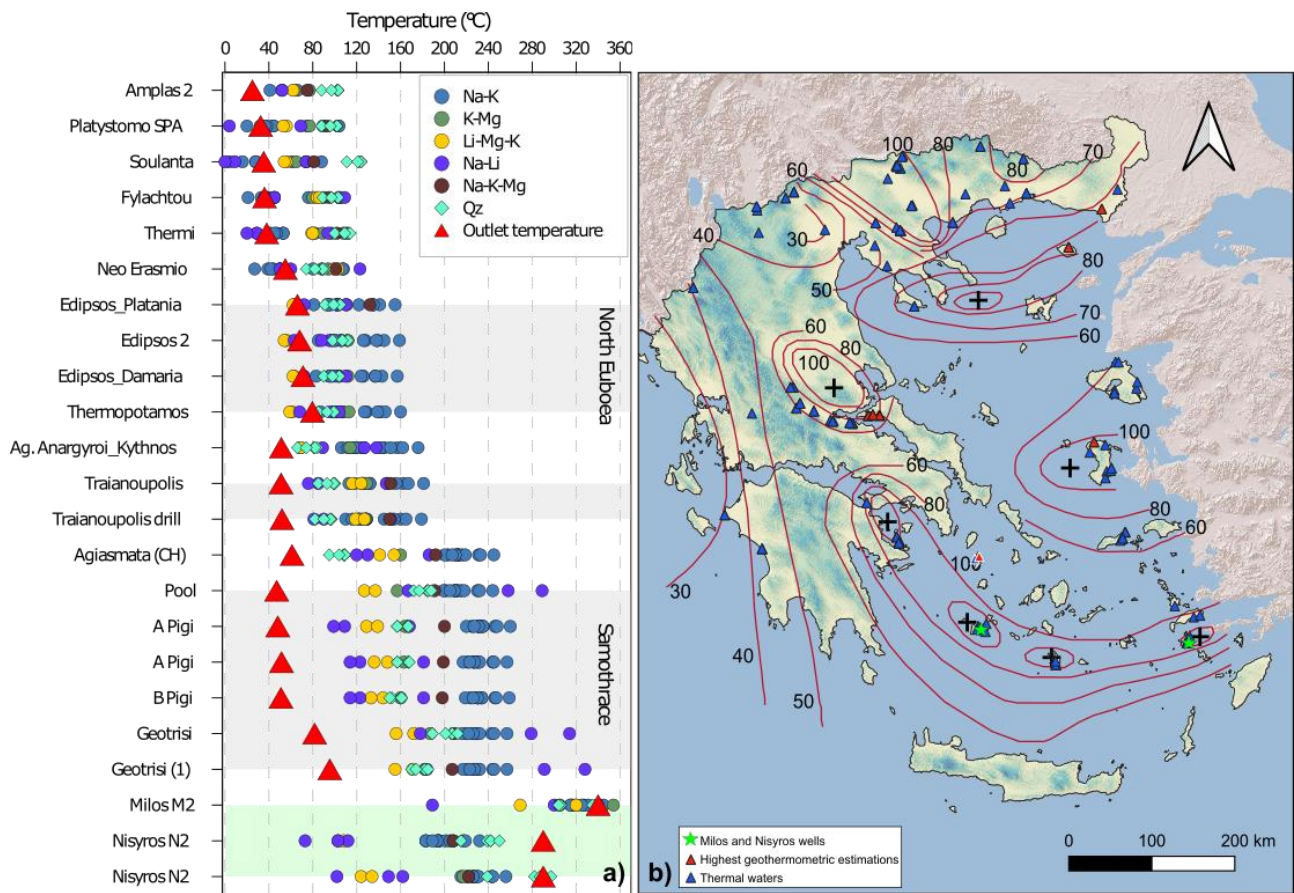


560 Fig. 79 - Triangular ~~diagram~~ diagrams of a) Cl-SO₄-HCO₃ (Giggenbach, 1991) and b) Na-K-Mg (Giggenbach, 1988).

Many of the partially equilibrated samples are close to the seawater point and thus, the temperature of the reservoir could not be estimated due to the contamination with marine water. Only a few partially equilibrated samples mostly from Samothraki Island and Edipsos area may be considered reliable indicating temperatures up to 240-260 °C (Geotrisi). All these sites were selected and compared to the temperatures obtained from other geothermometric equations using the software Solute Geothermometers (SolGeo – Verma et al., 2008), which estimates the minimum temperature of the aquifer by comparing thirty-five geothermometric equations (Fig. 810a). The geothermometric estimations made with this software are based on the solute concentrations of the sampled waters. Many empirical geothermometric equations have been proposed by different researchers during the years and have been grouped together in this program. Most of them are based on cationic contents of the waters: 13 equations are based on the Na⁺ and K⁺ contents of the waters, 3 on K⁺ and Mg²⁺, 2 on Li⁺ and Mg²⁺, 5 on Na⁺ and Li⁺, 3 on Na⁺, K⁺ and Ca²⁺, 1 on Na⁺, K⁺ and Mg²⁺, 2 on Na⁺, K⁺, Ca²⁺ and Mg²⁺ and finally 7 are silica geothermometers based on the SiO₂ content. For the references of these geothermometers we refer to the paper of Verma et al. (2008(2008) while the formulas are included as supplementary material (Table S2).

570

575



580 Fig. 8–10 – (a) Results of the geothermometric estimations made with the computer program SolGeo (Verma et al., 2008) on selected samples that plotted in the partial equilibration field of the Giggenbach diagram of Fig. 7–9. (b) Thermal waters plotted on heat flow map (mW/m^2) (Fytikas and Kolios, 1979); red triangular indicates the highest estimated temperatures from geothermometric equations.

As generally happens, the equations do not give back a unique temperature, but a wide range. The Na-K geothermometers show mostly the highest temperatures of reservoirs, with up to about 40 °C differences. On the contrary, Li-Mg-K and Na-Li geothermometers present the lowest results; sometimes below the outlet temperature of the spring. It should be mentioned that the Na-K geothermometers are considered the most reliable because less affected by mixing with shallow waters and degassing (Pope et al., 1987).

590 Excluding geothermometers giving estimations at or below the emergence temperature, the narrowest range is shown at thermal waters with estimated temperatures below 120 °C (Fig. 810a) and comprise samples from central Greece (Soulanta, Platystomo SPA and Amplas2) and from northeastern Greece (Thermi, Neo Erasmio and Fylachtou).

595 A few sites gave Na-K estimations up to 160-180 °C (Fig. 810a) indicating an important geothermal potential for the area of Edipsos (Northern Evia Island), Traianoupolis (Thrace) and Agioi Anargyroi (Kythnos Island). Only two areas gave estimations above 200 °C and up to 250 °C: the

areas of Therma on Samothraki Island and of Agiasmata on Chios Island. For these systems, further studies should ascertain if they might be used also for electricity production.

To support this hypothesis, Fig.10b evidences a correspondence among thermal springs and heat flux. The majority of studied thermal springs are located in areas with heat flux higher of 60 mW/m², whilst the highest values of temperature obtained from geothermometric estimation correspond to areas with elevated heat flow (> 80 mW/m²). The maxima of heat flux (> 120 mW/m²), found along the SAAVA, do not show thermal springs with high measured temperature or high geothermometric estimates. This does not mean that no high temperature geothermal system is present, but only that its impermeable seal is very efficient. As previously mentioned, in fact, two high enthalpy geothermal systems have been ascertained on the islands of Milos and Nisyros by explorative drillings. The geothermometric estimates made with the composition of the captured waters gave results closely resembling the measured temperature in the case of Milos (Fig. 10a). In the case of Nisyros the close correspondence between estimation and measured value is found only for the silica geothermometer (Fig. 10a), which is less influenced by the contamination of the seawater used for the drilling mud (Chiodini et al. 1993).

5.5 Tectonic structures as a fluid carrier

After studying the gas emissions of Greece, Daskalopoulou et al. (2018a) noticed a connection between lithological facies and dominant gas components. Particularly, the sedimentary regime of EH, where hydrocarbon deposits are present, yield that CH₄ and N₂ are the dominant gas species in the area. On the other hand, CO₂ is the principal gas component in IH and HH, where intrusive and metamorphic formations prevail. On the basis of the geographical distribution of the gases, a similar behaviour between CO₂ concentrations and R_C/R_A ratios is noticed (Daskalopoulou et al., 2018a; 2019a). This reflects increasing CO₂ and R_C/R_A values in areas characterized by thin crust, elevated heat flow values, Plio-Quaternary volcanic activity and deep routed extensional or transtensional regional faults (Fig. 2b) (Daskalopoulou et al., 2019a); VA displays a higher mantle contribution for both CO₂ and He with respect to EH that present an important crustal input (Daskalopoulou et al., 2019a).

As faults create a permeable pathway for gases to ascend (Wang and Jaffe, 2004) special attention was given to places with complex tectonics. In northern Greece, the Strymonas Fault System is controlling the tectonics. In this area, gases collected from thermal waters, present an up to 15% mantle contribution for He (considering a MORB end-member). This is likely caused due to the U- and Th-rich minerals (i.e. zircon, apatite etc - Wüthrich, 2009) of the granitoids present in this area; the decay of U and Th produces ⁴He thereafter depleting the R/R_A values. Gases collected from the

635 thermal waters of Euboea and Samothraki are found in the Grecian Shear Zone (propagation of the NAF towards the Hellenic mainland - Şengör, 1979). According to various authors (Güleç and Hilton, 2006; Güleç et al., 2002; Mutlu et al., 2008) almost more than 50 % of the He along some sections NAF derives from the mantle, hence R/R_A values are expected to be enriched in mantle He. Gases collected from the cold waters of Corinth Gulf are generally dominated by CH_4 and N_2 and the associated He shows always R/R_A values typical to pure crustal origin (Pik and Marty, 2009). The same authors explained that the fault system is not connected in depth with zones in which mantle He can be trapped or that reaches the lower crust allowing the uprise of mantle fluids. It is worth mentioning that in the western part of the graben system (Saronikos gulf), where it meets the SAAVA, the Quaternary volcanic activity of Sousaki and Methana allowed CO_2 -rich fluids to reach the surface.

640 The above described extensional and transtensional deep regional tectonic structures, which are permeable pathways to the earth's surface for mantle or deep crustal fluids, allow also deep circulation of groundwater creating the conditions for the formation of small hydrothermal systems.

645 In the case of the presence of an important heat source, along such tectonic structures some greater or higher temperature hydrothermal systems may form. This is the case of both Samothraki island and Edipsos (Fig. 10b) where the heat source is a Ternary granitic intrusion in the former case (Dotsika 2012) and a Quaternary volcanic system in the latter (D'Alessandro et al. 2014).

650 **Conclusions**

Thermo-mineral waters in Greece are strongly controlled by the geologic and geodynamic setting that characterises the area where they are found. On the basis of pH, hyperalkaline Ca-OH type waters were identified in the ophiolitic sequences of Argolida and Othrys, while acidic waters were documented on islands located along the SAAVA. The former group represents the evolution of waters in deep serpentinized ultramafic aquifers in conditions closed to the atmosphere, while the latter highlights the impact of the volcanic/geothermal degassing on the waters. Based on their temperature, the remaining samples were subdivided into cold and thermal. Cold waters found in the northern part of Greece showed high pCO_2 values and were characterised by Ca- HCO_3

655

660 composition. Carbon dioxide dissolution resulted in slightly acidic waters with elevated bicarbonate content. Saturation or oversaturation in the carbonate minerals is not common in this group. Few water samples with intermediate pCO_2 were saturated, while the lack of equilibrium with carbonate minerals underscored the importance of CO_2 dissolution. Cold waters collected in hydrocarbon prone areas of western Greece presented low pCO_2 and were close to equilibrium with the main

665 carbonate minerals suggesting that the petrological regime (sedimentary limestones) governs the
equilibrium of the dissolved carbonate species. On the other hand, thermal waters were seemingly
controlled by the high heat flow values and the low crustal thickness. Their chemical composition
was strongly influenced by mixing processes between meteoric water and seawater.
Geothermometry was applicable only in few partially equilibrated waters suggesting reservoir
670 temperatures from 80 °C to 260 °C with the most elevated values (between 200 °C and 260 °C)
being found in two islands of the eastern Aegean Sea: [\(Samothraki and Chios\)](#).

This extensive dataset represents an almost complete catalogue of hydrogeochemical data on
thermo-mineral waters of whole Greece. It has been gathered over 15 years by the same research
group and analysed in the same laboratory ensuring a good analytical uniformity. This database
675 represents therefore a good basis for future studies on the thermo-mineral waters of this country.

Acknowledgements

We kindly acknowledge all the Greek colleagues that helped us either in the field or with precious
information about the sampling sites. Among them we remember K. Athanasoulis, E. Dotsika, N.
680 Lambrakis, S. Karakatsanis, K. Katsanou, N. Kolios, M. Margaritopoulos, G. Michas, G. Papadakis
and M. Xenakis. Precious help either in the field or in the laboratory came also from S. Bellomo, C.
Bruno, L. Brusca, G. Capasso, S. Francofonte, F. Grassa, M. Liotta, M. Minio, Y. Oliveri, F.
Plicanti, V. Prano, A. Sollami, G. Volpicelli. We are also extremely grateful to all the owners,
managers, public officers and employees, who gave us access to and precious information about the
685 sampling points and/or helped us in the sampling operations. [We are indebted to two anonymous
reviewers whose insightful comments helped us to improve this paper.](#)

Declaration

No specific funding was received for conducting this study. We acknowledge the support of Istituto
690 Nazionale di Geofisica e Vulcanologia for all the analyses made for free in their laboratories.

References

Andritsos, N., Dalambakis, P., Arvanitis, A., Papachristou, M., & Fytikas, M. (2015). Geothermal
Developments in Greece – Country update 2010-2014. Proceedings World Geothermal
695 Congress 2015. Melbourne, Australia, 19-25.

- APHA, AWWA, WEF (2005). *Standard Methods for the Examination of Water and Wastewater*, 21st ed. American Public Health Association, Washington D.C., U.S.A.
- Argiriou, A.A., & Lykoudis, S.P. (2006). Isotopic composition of precipitation in Greece. *Journal of Hydrology*, 327, 486-495.
- 700 Athanasoulis, K., Vakalopoulos, P., Xenakis, M., Persianis, D., & Taktikos, S. (2009). *Periodic monitoring of spa sources of Greece*. Project Report “Integrated quantitative and qualitative study of the thermomineral waters of the country” Institute of Geological and Mineral Exploration (IGME) Athens (in Greek)
- Barnes, I., Lamarche, V.C., & Himmelberg, G. (1967). Geochemical evidence of present-day
705 serpentinization. *Science*, 159, 830-832.
- Brombach, T., Caliro, S., Chiodini, G., Fiebig, J., Hunziker, J., Raco, B. (2003). Geochemical evidence for mixing of magmatic fluids with seawater, Nisyros hydrothermal system, Greece. *Bulletin of Volcanology*, 65(7), 505–516
- Bruni, J., Canepa, M., Chiodini, G., Cioni, R., Cipolli, F., Longinelli, A., Marini, L., Ottonello, G.,
710 & Vetuschi Zuccolini, M. (2002). Irreversible water–rock mass transfer accompanying the generation of the neutral, Mg–HCO₃ and high-pH, Ca–OH spring waters of the Genova province, Italy. *Applied Geochemistry*, 17, 455–474.
- Chiodini, G., Cioni, R., Leonis, C., Marini, L., & Raco, B. (1993). Fluid geochemistry of Nisyros Island, Dodecanese, Greece. *Journal of Volcanology and Geothermal Research*, 56, 95–112
- 715 Chiodini, G., Frondini, F., & Ponziani, F. (1995). Deep structures and carbon dioxide degassing in Central Italy. *Geothermics*, 24, 81–94.
- Chiodini, G., Cioni, R., Di Paola, G.M., Dotsika, E., Fytikas, M., Guidi, M., Leonis, C., Lyberopoulou, V., Magro, G., Marini, L., Meletidis, S., Michelot, J.L., Poutoukis, D., Raco, B., Russo, M., Virgili, G. (1998). Geochemistry of Santorini fluids, European Commission. *Volcanic risk. The European laboratory volcanoes*, in: R. Casale, M. Fytikas, G. Sigvaldasson, G. Vougioukalakis (Eds.) *Proceedings of the Second Workshop. Santorini, Greece 2-4 May 1996*, EUR 18161 EN,193-232.
- 720
- Cipolli, F., Gambardella, B., Marini, L., Ottonello, G., & Vetuschi Zuccolini, M. (2004). Geochemistry of high-pH waters from serpentinites of the Gruppo di Voltri (Genova, Italy) and
725 reaction path modeling of CO₂ sequestration in serpentinite aquifers. *Applied Geochemistry*, 19, 787–802.
- Clayton, R.N., O’Neil, J.R., & Mayeda, T.K. (1972). Oxygen isotope exchange between quartz and water. *Journal of Geophysical Research*, 77, 3057-3067
- Craig, H. (1961). Isotopic variation in meteoric waters. *Science*, 133, 1702–1703.

- 730 D'Alessandro, W., Brusca, L., Kyriakopoulos, K., Michas, G., & Papadakis, G. (2009). Hydrogen sulphide as a natural air contaminant in volcanic/geothermal areas: the case of Sousaki, Corinthia (Greece). *Environmental Geology*, 57(8), 1723–1728.
- D'Alessandro, W., Bellomo, S., Brusca, L., Karakazanis, S., Kyriakopoulos, K., & Liotta, M. (2011). The impact on water quality of the high carbon dioxide contents of the groundwater in the area of Florina (N. Greece). In: *Advances in the Research of Aquatic Environment* (Lambrakis, N., Stournaras, G., Katsanou, K. eds.) Springer, Berlin, Germany, vol. 2, 135-143
- 735 D'Alessandro, W., Brusca, L., Kyriakopoulos, K., [Michas, G. & Papadakis, G. \(2008\). Methana, the westernmost active volcanic system of the south Aegean arc \(Greece\): insight from fluids geochemistry. *Journal of Volcanology and Geothermal Research*, 178, 818–828](#)
- 740 D'Alessandro, W., Brusca, L., Kyriakopoulos, K., Bellomo, S., & Calabrese, S. (2014). A geochemical traverse along the “Sperchios Basin - Evoikos Gulf” Graben (Central Greece): origin and evolution of the emitted fluids. *Marine and Petroleum Geology*, 55, 295-308.
- D'Alessandro, W., [Bellomo, S., Brusca, L., Kyriakopoulos, K., Calabrese, S. & Daskalopoulou, K. \(2017\). The impact of natural and anthropogenic factors on groundwater quality in an active volcanic/geothermal system under semi-arid climatic conditions: The case study of Methana peninsula \(Greece\). *Journal of Geochemical Exploration*, 175, 110–119](#)
- 745 D'Alessandro, W., Daskalopoulou, K., Calabrese, S., & Bellomo, S. (2018). Water chemistry and abiogenic methane content of a hyperalkaline spring related to serpentinization in the Argolida ophiolite (Ermioni, Greece). Special issue on gas geochemistry (Zhang S. and Yüce G. eds.), *Marine and Petroleum Geology*, 89, 185-193.
- 750 [Daskalaki, P., & Voudouris, K. \(2008\). Groundwater quality of porous aquifers in Greece: a synoptic review. *Environmental Geology*, 54, 505-513.](#)
- Daskalopoulou, K., Calabrese, S., Grassa, F., Kyriakopoulos, K., Parello, F., Tassi, F., & D'Alessandro, W. (2018a). Origin of methane and light hydrocarbons in natural fluid emissions: a key study from Greece. *Chemical Geology*, 479, 286-301.
- 755 Daskalopoulou, K., Gagliano, A.L., Calabrese, S., Longo, M., Hantzis, K., Kyriakopoulos, K., & D'Alessandro, W. (2018b). Gas geochemistry and CO₂ output estimation of the Island of Milos, Greece. *Journal of Volcanology and Geothermal Research*, 365, 13–22, doi: 10.1016/j.jvolgeores.2018.10.003
- 760 Daskalopoulou, K., Calabrese, S., Gagliano, A.L., & D'Alessandro, W. (2019a). Estimation of the geogenic carbon degassing of Greece. *Applied Geochemistry*, 106, 60-74.
- Daskalopoulou, K., Gagliano, A.L., Calabrese, S., Li Vigni, L., Longo, M., Kyriakopoulos, K., Pecoraino, G., & D'Alessandro, W. (2019b). Degassing at the volcanic/geothermal system of

- Kos (Greece): geochemical characterization of the released gases and CO₂ output estimation. *Geofluids*, Volume 2019, Article ID 3041037, doi: 10.1155/2019/3041037
- 765
- Drever, J.L. (1982). *The Geochemistry of Natural Waters*. Prentice-Hall, Englewood Cliffs, NJ, USA, pp. 82-85.
- [Dolgorjav, O. \(2009\) Geochemical characterization of thermal fluids from the Khangay area, Central Mongolia. Geothermal training programme reports, Orkustofnun, Grensásvegur, 9.](#)
- 770
- Dotsika, E. (2012). Isotope and hydrochemical assessment of the Samothraki Island geothermal area, Greece. *Journal of Volcanology and Geothermal Research* 233-234, 18–26
- [Doutsos, T., Koukouvelas, I.K., & Xypolias, P. \(2006\). A new orogenic model for the External Hellenides. Geological Society, London, Special Publications, 260, 507-520, doi.org/10.1144/GSL.SP.2006.260.01.21.](#)
- 775
- Duriez, A., Marlin, C., Dotsika, E., Massult, M., Noret, A., & Morel, J.L. (2008). Geochemical evidence of seawater intrusion into a coastal geothermal field of central Greece: example of the Thermopylae system. *Environmental Geology*, 54, 551-564. DOI 10.1007/s00254-007-0857-9.
- Evans, B.W., Hattori, K., & Baronnet, A. (2013). Serpentinite: what, why, where? *Elements*, 9, 99–106.
- 780
- Fytikas, M. (1988). Geothermal situation in Greece. *Geothermics*, 17, 549-556.
- Fytikas, M., & Kolios, N. (1979). Preliminary heat flow map of Greece. In: Cermak V., Rybach L., (Eds.), *Terrestrial Heat Flow in Europe*. Springer-Verlag, Berlin Heidelberg New York, pp. 197-205.
- Fytikas, M., Innocenti, F., Manetti, P., Mazuoli, R., Peccerilo, A., & Villari, L. (1984). Tertiary to
- 785
- Quaternary evolution of the volcanism in Aegean Sea. In: Dixon J.E., Robertson AHF (eds). *The geological evolution of the Eastern Mediterranean*, vol 17, 687-699. (Geol. Soc. London Spec. Pub.).
- Fytikas, M., Margomenou-Leonidopoulou, G., & Cataldi, R. (1999). Geothermal Energy in Ancient Greece: From Mythology to Late Antiquity. In: *Stories from a Heated Earth*. Geothermal
- 790
- Resources Council and IGA, California.
- Fytikas, M., Andritsos, N., Dalabakis, P., & Kolios, N. (2005). Greek geothermal update 2000–2004. In: *Proceedings World Geothermal Congress 2005*, Antalya, Turkey, 24–29 Apr 2005.
- Gat, J.R., & Carmi, H. (1971). Evolution of the isotopic composition of atmospheric waters in the Mediterranean Sea area. *Journal of Geophysical Research*, 75, 3039–3040.
- 795
- Giggenbach, W.F. (1988). Geothermal solute equilibria. Derivation of Na-K-Mg-Ca geothermometers. *Geochimica et Cosmochimica Acta*, 52(12), 2749–2765.

- 800 Giggenbach, W.F. (1991). Chemical techniques in geothermal exploration. In: D'Amore, F. (Ed.), *Application of Geochemistry in Geothermal Reservoir Development*. UNITAR/UNDP, Rome, 252–270.
- Gilhooly III, W.P., Fike, D.A., Druschel, G.K., Kafantaris, F.C.A., Price, R.E. & Amend, J.P. (2014). Sulfur and oxygen isotope insights into sulfur cycling in shallow-sea hydrothermal vents, Milos, Greece. *Geochemical Transactions*, 15, 12
- Grigoriadis, V., Tziavos, I., Tsokas, G., & Stampolidis, A. (2016). Gravity data inversion for Moho depth modeling in the Hellenic area. *Pure and Applied Geophysics*, 173, 1223–1241.
805 DOI:10.1007/s00024-015-1174-y.
- Güleç, N., Hilton, D.R., & Mutlu, H. (2002). Helium isotope variations in Turkey: relationship to tectonics, volcanism and recent seismic activities. *Chemical Geology*, 187, 129-142.
- Güleç, N.H., & Hilton, D.R., (2006). Helium and heat distribution in western Anatolia, Turkey: Relationship to active extension and volcanism. In: Dilek, Y., Pavlides, S., (Eds).
810 *Postcollisional Tectonics and Magmatism in the Mediterranean Region and Asia. In: Geological Society of America Special Papers*, 409, 305–319.
- Håland, E.J. (2009). Water Sources and the Sacred in Modern and Ancient Greece and Beyond. *Water History*, 1, 83-108.
- Kallioras, A., & Marinos, P. (2015) Water resources assessment and management of karst aquifer
815 *systems in Greece. Environmental Earth Sciences*, 74, 83-100.
- Karakatsanis, S., Koukouzas, N., Pagonas, M., & Zelilidis, A. (2007). Preliminary sedimentological results indicate a new detailed stratigraphy for the Florina sedimentary basin and relate them with CO₂ presence. *Bulletin of the Geological Society of Greece*, 40, Proc. 11th Internat. Congr., Athens, May 2007
- 820 Karolyte, R., Serno, S., Johnson, G., & Gilfillan, S.M.V. (2017). The influence of oxygen isotope exchange between CO₂ and H₂O in natural CO₂-rich spring waters: implications for geothermometry. *Applied Geochemistry*, 84, 173–186.
- Kaya, E., Zarrouk, S.J., & O'Sullivan, M.J. (2011). Reinjection in geothermal fields: a review of worldwide experience. *Renewable and Sustainable Energy Reviews*, 15, 47–68.
- 825 Kharaka, Y.K., & Mariner, R.H. (1989). Chemical geothermometers and their application to formation waters from sedimentary basins, in: Naeser, N.D. and McCollon, T.H. (eds.), *Thermal History of Sedimentary Basins: Springer-Verlag, New York*, pp. 99-1 17.
- Koutroupis, N. (1992). Update of geothermal energy development in Greece. *Geothermics*, 21, 881-890.

- 830 Lambrakis, N., & Kallergis, G. (2005). Contribution to the study of Greek thermal springs: hydrogeological and hydrochemical characterized and origin of the thermal waters. *Hydrogeology Journal*, 13, 506-521.
- Landerer, X. (1843). *Beschreibung der heilquellen Griechenlands*. Nürnberg.
- Langelier, W., Ludwig H. (1942). Graphical methods for indicating the mineral character of natural
835 waters. *JWWA*, 34, 335-352
- Le Pichon, X., Sengor, A.M.C., Demirbag, E., Rangin, C., Imren, C., Armijo, R., Gorur, N., Cagatay, N., Mercier de Lépinay, M., Meyer, B., Saatcilar, B., & Tok, B. (2001). The active Main Marmara fault. *Earth and Planetary Science Letters*, 192, 595–616
- Liakopoulos, A., Katerinopoulos, A., Markopoulos, T., & Boulegue, J. (1991). A mineralogical
840 petrographic and geochemical study of samples from wells in the geothermal field of Milos island (Greece). *Geothermics*, 20, 237–256.
- Li Vigni, L., Daskalopoulou, K., Calabrese, S., Parello, F., & D'Alessandro, W. (2020/2021). Geochemical characterisation of the alkaline and hyperalkaline groundwater in the Othrys Ophiolite Massif, central Greece. *Italian Journal of Geosciences*, [140\(1\), 42-56](#), doi:10.3301/IJG.2020.
845
- Machel, H.G. (2001). Bacterial and thermochemical sulfate reduction in diagenetic settings — old and new insights. *Sedimentary Geology* 140, 143–175
- Marini, L., & Fiebig, J. (2005). Fluid geochemistry of the magmatic-hydrothermal system of Nisyros (Greece), *Mémoire de Géologie*, 44, 192.
- 850 [Marini, L., Gambardella, B., Principe, C., Arias, A., Brombach, T., & Hunziker, J.C. \(2002\). Characterization of magmatic sulfur in the Aegean island arc by means of the \$\delta^{34}\text{S}\$ values of fumarolic \$\text{H}_2\text{S}\$, elemental S, and hydrothermal gypsum from Nisyros and Milos islands. *Earth Planetary Science Letters*, 200, 15–31.](#)
- McClusky, S., Balassanian, S., Barka, A., Demir, C., Ergintav, S., Georgiev, I., Gurkan, O.,
855 Hamburger, M., Hurst, K., Kahle, H., Kastens, K., Kekelidze, G., King, R., Kotzev, V., Lenk, O., Mahmoud, S., Mishin, A., Nadariya, M., Ouzounis, A., Paradissis, D., Peter., Y., Prilepin, M., Reilinger, R., Sanli, I., Seeger, H., Tealeb, A., Toksöz, M.N., & Veis, G. (2000). Global Positioning System constraints on plate kinematics and dynamics in the Eastern Mediterranean and Caucasus. *Tectonophysics*, 105, 5695–5719.
- 860 Mendrinou, D., Choropanitis, I., Polyzou, O., & Karytsas, C. (2010) Exploring for geothermal resources in Greece. *Geothermics*, 39, 124-137 doi:10.1016/j.geothermics.2009.11.002

- Mercier, J.L. (1981). Extensional-compressional tectonics associated with the Aegean Arc: comparison with the Andean Cordillera of south Peru-north Bolivia. *Philosophical Transactions of the Royal Society London*, A300, 337-355.
- 865 [Meyback, M. \(1987\). Global chemical weathering of surficial rocks estimated from river-dissolved loads. *American Journal of Science*, 287, 401–428.](#)
- Minissale, A., Duchi, V., Kolios, N., & Totaro, G. (1989). Geochemical characteristics of Greek thermal springs. *Journal of Volcanology and Geothermal Research*, 39, 1-16.
- Minissale, A., Duchi, V., Kolios, N., Nocenti, M., & Verruchi, C. (1997). Chemical patterns of the
870 thermal aquifers in the volcanic Islands of the Aegean Arc, Greece. *Geothermics*, 26(4), 501–518.
- Mountrakis, D.M. (1985). *Geology of Greece*. University Studio Press, Thessaloniki, pp. 207 (in Greek).
- Mountrakis, D.M. (2010). *Geology and geotectonic evolution of Greece*. University Studio Press,
875 Thessaloniki, pp. 374 (in Greek).
- [Mutlu, H., Güleç, N., & Hilton, D.R. \(2008\). Helium–carbon relationships in geothermal fluids of western Anatolia, Turkey. *Chemical Geology*, 247, 305-321.](#)
- Nordstrom, D.K., McCleskey R.B., & Ball, J.W. (2009). Sulfur geochemistry of hydrothermal waters in Yellowstone National Park: IV acid-sulfate waters. *Applied Geochemistry*, 24, 191-
880 207.
- NTO/National Touring Organisation (1966). Bathing sites and curative springs. National Printing Office, Athens. (In Greek, with extended summaries in French and English).
- Palacas, J.G., Monopolis, D., Nicolaou, C.A., & Anders, D.E. (1986). Geochemical correlation of surface and subsurface oils, western Greece. *Organic Geochemistry* 10, 417–423.
- 885 Papachristou, M., Arvanitis, A., Mendrinou, D., Dalambakis, P., Karytsas, C., & Andritsos, N. (2019). Geothermal Energy Use, Country Update for Greece (2016-2019). *Proceedings of the European Geothermal Congress 2019*, Den Haag, The Netherlands, 11-14 June 2019.
- Parkhurst, D.I., & Appelo, C.A.J. (1999). *User guide to PHREEQC (Version 2) – a computer program for speciation, batch-reaction, one-dimensional transport, and inverse geochemical
890 calculation*. U.S. Geol. Surv. Water Resour. Invest. Rep. 99-4259, p. 310.
- Pavlidis, S., & Caputo, R. (2004). Magnitude versus faults’ surface parameters: quantitative relationships from the Aegean. *Tectonophysics*, 380, 3-4, 159-188
- Pavlidis, S.B., & Mountrakis, D.M. (1987). Extensional tectonics of northwestern Macedonia, Greece, since the late Miocene. *Journal of Structural Geology*, 9, 385-392

- 895 Pavlides, S., Caputo, R., Sboras, S., Chatzipetros, A., Papathanasiou, G., & Valkaniotis, S., 2010. The Greek catalogue of active faults and database of seismogenic sources. *Bulletin of the Geological Society of Greece*, 43 (1), 486–494.
- Pearce, JM (Ed.) (2004). *Natural analogues for the geological storage of CO₂*. Final report of the Nascent project. British Geological Survey Technical Report, 122 pp
- 900 Pe-Piper, G., & Piper, D.J.W. (2002). *The igneous rocks of Greece, The anatomy of an orogen*. Beiträge zur regionalen Geologie der Erde 30, Gebrüder Bornträger, Berlin - Stuttgart.
- Pe-Piper, G., & Piper, D.J.W. (2006). Unique features of the Cenozoic igneous rocks of Greece. *Geological Society of America, Special Paper* 409, 259- 282.
- Pertessis, M. (1937). *Thermomineral Springs of Greece*. Publication of the Geological Survey of Greece, n. 24. Athens (in Greek).
- 905 Pik, R., & Marty, B. (2009). Helium isotopic signature of modern and fossil fluids associated with the Corinth rift fault zone (Greece): Implication for fault connectivity in the lower crust, *Chemical Geology*, 266, 67-75.
- Pollack, H.N., Hurter, S., & Johnson, J.R. (1993). Heat Flow from the Earth's Interior: Analysis of the Global Data Set. *Reviews of Geophysics*, 31, 267-280
- 910 Pope, L.A., Hajash, A., & Popp, R.K. (1987). An experimental investigation of the quartz, Na–K, Na–K–Ca geothermometers and the effects of fluid composition. *Journal of Volcanology and Geothermal Research* 31, 151–161.
- Rezaei, A., Javadi, H., Rezaeian, M., & Barani, S. (2018). Heating mechanism of the Abgarm–Avaj geothermal system observed with hydrochemistry, geothermometry, and stable isotopes of thermal spring waters, Iran. *Environmental Earth Sciences* 77, 635
- 915 Rigakis, N., & Karakitsios, V. (1998). The source rock horizons of the Ionian Basin (NW Greece). *Marine and Petroleum Geology* 15, 593–617
- Sengör, A.M.C. (1979). The North Anatolian Transform Fault: its age, offset and tectonic significance. *Journal of Geological Society of London* 136, 269–82.
- 920 Sinclair, A.J. (1974). Selection of threshold values in geochemical data using probability graphs. *Journal of Geochemical Exploration*, 3, 129-149.
- Singh, H., Chandrasekharam, D., Vaselli, O., Trupti, G., Singh, B., Lashin, A. & Arifi, N.A. (2015). Physico-chemical characteristics of Jharkhand and West Bengal thermal springs along SONATA mega lineament, India. *Journal of Earth System Science*, 124(2), 419–430.
- 925 Taymaz, T., Jackson, J., & McKenzie, D. (1991). Active tectonics of the north and central Aegean Sea. *Geophysical Journal International*, 106, 433–90.

- 930 Tsokas, G.N., & Hansen, R.O., (1997). Study of the crustal thickness and the subducting lithosphere in Greece from gravity data. *Journal of Geophysical Research*, 102 (B9), 585–597. doi:10.1029/97JB00730.
- van Hinsbergen, D.J.J., Hafkenscheid, E., Spakman, W., Meulenkamp, J.E., & Wortel, R. (2005). Nappe stacking resulting from subduction of oceanic and continental lithosphere below Greece. *Geology*, 33(4), 325–328.
- 935 Verma, S.P., Pandarinath, K., & Santoyo, E. (2008). SolGeo: A new computer program for solute geothermometers and its application to Mexican geothermal fields. *Geothermics*, 37, 597–621
- Vougioukalakis, G., Eleftheriadis, G., Christofides, G., Pavlides, S., Fytikas, M., & Villa, I. (2004). Volcanological study of the Almopias Pliocene volcanic formations (N Greece). *Proceedings of the 5th International Symposium on Eastern Mediterranean Geology* 3, 1318–1321.
- 940 Wang, S. & Jaffe, P.R. (2004). Dissolution of a mineral phase in potable aquifers due to CO₂ releases from deep formations. *Effect of dissolution kinetics Energy Conversion and Management*, 45, 2833-2848.
- Wüthrich, E.D. (2009). Low temperature thermochronology of the northern Aegean Rhodope Massif. Doctor of Sciences Thesis, Swiss Federal Institute of Technology Zurich, Switzerland.

ID	Sample	Sector	Coordinates		Altitude	Date	References	Location	Zone	Sigla	T	pH	cond	Eh	Ca	Mg	Na	K	Alk	F	Cl	NO ₃	SO ₄	SiO ₂	Br	Li	NH ₄	Ionic Balance		TDS	δ ¹⁸ O	δD	d
			°C	μS/cm																								mV	mg/l				
412	Kos Aspro Nero	35S	522022	4078878	314	#####		Kos	Attico-Cycladic	VA	13.9	4.70	1530	331	272	103	21.5	10.0	bdl	1.7	39.8	1.9	1234	29.9	bdl	66.2	0.18	-14.4	1821	-5.3	-23	19.1	
414	Kos Kokkino Nero 3	35S	522105	4078817	343	#####		Kos	Attico-Cycladic	VA	23.2	3.37	2400	275	507	157	26.8	25.2	bdl	1.8	41.3	1.7	2716	50.2	bdl	85.2	1.75	-36.3	3749	-10.0	-26	53.7	
413	Kos Kokkinonero 2	35S	522116	4078886	320	#####		Kos	Attico-Cycladic	VA	20.3	3.09	3000	111	508	257	29.2	10.6	bdl	2.4	45.0	1.6	2775	41.0	bdl	56.9	0.41	-20.6	3840	-7.5	-25	34.9	
580	Paleochori cave	35S	277771	4061595	0	6/9/2017		Milos	Attico-Cycladic	VA	75.3	2.85	70000	-40	1147	1165	14900	1825	bdl	bdl	29707	bdl	2313	117	bdl	11278	11.9	-4.4	62537	n.d.	n.d.	n.d.	
287	Stefanos	35S	515058	4048069	86	9/3/2009		Nisyros	Attico-Cycladic	VA	98.0	1.96	6000	-30	32.0	10.9	26.3	45.3	bdl	0.5	7.9	bdl	2786	332	bdl	9.7	23.3	-169.6	3379	n.d.	n.d.	n.d.	

ID	Sample	Sector	Coordinates		Altitude	Date	References	Site	Location	Zone	Sigla	T	pH	cond	Eh	Ca	Mg	Na	K	Alk	F	Cl	NO ₃	SO ₄	SiO ₂	Br	Li	NH ₄	Ionic Balance	TDS	δ ¹⁸ O	δD	d
			E	N																													
193	Archani	34S	600606	4315575	176	#####	D'Alessandro et al., 2014	Achani	Sperchios	Subpelagionian	IH	27.5	11.2	570	-235	35.9	0.122	22.8	0.78	146	0.02	14.5	bdl	0.48	5.8	0.1	0.32	n.d.	-0.4	228	-8.6	-60	8.0
266	Archani	34S	600613	4315572	202	#####	D'Alessandro et al., 2014	Achani	Sperchios	Subpelagionian	IH	27.6	11.3	538	-258	35.7	0.122	23.2	0.78	153	0.01	17.4	bdl	0.96	5.3	0.1	0.29	n.d.	-6.5	237	-8.9	-58	13.4
406	Archani	34S	600613	4315572	202	9/6/2013	Li Vigni et al., 2021	Achani	Sperchios	Subpelagionian	IH	27.5	11.3	1090	-209	35.0	0.010	22.1	0.79	159	0.01	16.7	bdl	0.39	5.0	0.1	0.41	n.d.	-12.1	240	-8.3	-59	7.0
474	Archani	34S	600613	4315572	202	#####	Li Vigni et al., 2021	Achani	Sperchios	Subpelagionian	IH	27.7	11.4	589	-29	34.2	0.005	22.1	0.99	139	0.02	15.5	0.1	0.06	4.9	0.1	0.31	<0.01	-1.0	218	-9.7	-60	18.1
546	Archani	34S	600604	4315570	194	#####	Li Vigni et al., 2021	Achani	Sperchios	Subpelagionian	IH	27.3	11.3	525	-164	34.4	0.004	22.4	0.61	141	bdl	15.1	bdl	0.43	5.2	bdl	0.19	n.d.	-1.5	220	-8.8	-58	12.2
548	Archani 159	34S	600571	4315552	204	#####	Li Vigni et al., 2021	Achani	Sperchios	Subpelagionian	IH	26.6	11.4	497	-202	33.5	1.13	22.5	0.66	123	bdl	15.3	bdl	0.43	11.8	bdl	0.37	n.d.	11.6	210	-8.7	-58	11.4
549	Archani 160	34S	600579	4315550	203	#####	Li Vigni et al., 2021	Achani	Sperchios	Subpelagionian	IH	26.4	11.2	526	-327	35.7	0.001	22.8	0.66	143	bdl	17.4	bdl	0.24	9.8	bdl	0.32	n.d.	-1.9	231	-8.8	-60	10.3
529	Archani drill	34S	601328	4315973	239	#####	Li Vigni et al., 2021	Achani	Sperchios	Subpelagionian	IH	22.0	11.3	450	-30	45.8	0.007	10.6	0.51	130	bdl	28.9	bdl	0.08	1.6	0.2	0.17	n.d.	-6.7	218	-7.9	n.d.	n.d.
544	Archani drill	34S	601327	4315970	240	#####	Li Vigni et al., 2021	Achani	Sperchios	Subpelagionian	IH	22.2	11.4	525	n.m.	48.9	0.003	11.0	0.34	132	bdl	29.6	bdl	0.77	1.6	bdl	0.14	n.d.	-2.8	224	-8.1	-58	6.4
543	Kamaroules	34S	601018	4315720	222	#####	Li Vigni et al., 2021	Achani	Sperchios	Subpelagionian	IH	19.4	11.5	490	-124	41.9	0.027	12.8	0.34	135	bdl	19.1	bdl	1.44	0.9	bdl	0.09	n.d.	-4.3	212	-8.5	-57	10.6
243	Ekkara	34S	602784	4334991	167	#####	Li Vigni et al., 2021	Ekkara	Central GR	Subpelagionian	IH	22.6	11.3	764	-384	24.6	0.377	11.4	1.65	189	0.28	98.9	bdl	15.1	40.6	0.4	3.03	n.d.	0.7	489	-9.6	-66	11.0
475	Ekkara	34S	602820	4334018	198	#####	Li Vigni et al., 2021	Ekkara	Central GR	Subpelagionian	IH	25.2	11.5	463	-61	41.7	0.002	16.3	0.70	142	0.01	17.3	0.1	0.65	1.5	0.1	0.57	<0.01	-0.9	221	-9.3	-58	17.0
540	Ekkara	34S	602820	4334018	184	5/9/2017	Li Vigni et al., 2021	Ekkara	Central GR	Subpelagionian	IH	25.4	11.3	541	-270	42.1	0.003	16.6	0.46	145	bdl	17.2	bdl	5.52	1.6	bdl	0.39	n.d.	-5.1	229	-9.5	-64	11.7
537	Ekkara Ps	34S	602786	4334990	156	5/9/2017	Li Vigni et al., 2021	Ekkara	Central GR	Subpelagionian	IH	23.8	11.2	710	-317	15.4	0.132	11.2	1.62	173	0.19	91.1	bdl	10.5	40.3	0.3	3.23	n.d.	1.3	449	-8.9	-63	8.4
538	Kato Pasali	34S	602601	4334825	174	5/9/2017	Li Vigni et al., 2021	Ekkara	Central GR	Subpelagionian	IH	18.8	11.3	464	-159	37.9	0.739	33.4	1.04	117	bdl	24.4	1.7	16.0	25.5	bdl	1.75	n.d.	14.5	260	-8.9	-62	9.1
539	Psoroneria	34S	602618	4334806	171	5/9/2017	Li Vigni et al., 2021	Ekkara	Central GR	Subpelagionian	IH	23.8	11.3	632	-370	29.4	0.000	61.5	1.38	180	bdl	40.9	bdl	1.83	16.8	0.2	1.19	n.d.	0.9	334	-9.2	-65	8.8
483	Agia Anargyroi	34S	695941	4138821	46	#####	D'Alessandro et al., 2018	Ermioni	Argolis	Subpelagionian	IH	20.0	11.8	1200	33	75.7	0.038	67.1	10.14	278	bdl	73.6	7.9	2.98	0.8	0.2	41.4	5.4	2.1	563	-5.1	-31	9.4
484	Agia Anargyroi 2	34S	695943	4138808	53	#####	D'Alessandro et al., 2018	Ermioni	Argolis	Subpelagionian	IH	17.4	12.0	1440	44	93.0	0.052	64.9	8.97	388	bdl	67.9	2.4	1.30	0.1	0.2	40.5	6.1	-8.0	674	-5.4	-31	11.9

[Click here to view linked References](#)

Geothermometer	Acronym
Na–K	TNKFT73
Na–K	TNKT76
Na–K	TNKF79
Na–K	TNKT80
Na–K	TNKA83
Na–K	TNK2A83
Na–K	TNKNN87
Na–K	TNKG88
Na–K	TNKVS97
Na–K	TNKA00
Na–K	TNKC02
Na–K	TNKDSR08
Na–K	TNK2DS08
K–Mg	TKMG88
Li–Mg	TLMKM89
Li–Mg	TLM2KM89
Na–Li	TNLFM81
Na–Li	TNL2FM81
Na–Li	TNLKM89
Na–Li	TNLVS97
Na–Li	TNL2VS97
Na–K–Mg	TNKMNN87
Quartz	TSF77
Quartz	TS2F77
Quartz	TSFP82
Quartz	TSVS97
Quartz	TS2A00
Quartz	TSV00

Author

Na–K geothermometer of Fournier and Truesdell -1973

Na–K geothermometer of Truesdell -1976

Na–K geothermometer of Fournier -1979

Na–K geothermometer of Tonani -1980

Na–K geothermometer-1 of Arnórsson et al. -1983

Na–K geothermometer-2 of Arnórsson et al. -1983

Na–K geothermometer of Nieva and Nieva -1987

Na–K geothermometer of Giggenbach -1988

Na–K geothermometer of Verma and Santoyo -1997

Na–K geothermometer of Arnórsson -2000

Na–K geothermometer of Can -2002

Na–K geothermometer-1 of Díaz-González et al. (in press)

Na–K geothermometer-2 of Díaz-González et al. (in press)

K–Mg geothermometer of Giggenbach -1988

Li–Mg geothermometer-1 of Kharaka and Mariner -1989

Li–Mg geothermometer-2 of Kharaka and Mariner -1989

Na–Li geothermometer-1 of Fouillac and Michard -1981

Na–Li geothermometer-2 of Fouillac and Michard -1981

Na–Li geothermometer-1 of Kharaka and Mariner -1989

Na–Li geothermometer-1 of Verma and Santoyo -1997

Na–Li geothermometer-2 of Verma and Santoyo -1997

Na–K–Mg geothermometer of Nieva and Nieva -1987

Quartz geothermometer-1 of Fournier -1977

Quartz geothermometer-2 of Fournier -1977

Quartz geothermometer of Fournier and Potter II -1982

Quartz geothermometer-1 of Verma and Santoyo -1997

Quartz geothermometer-2 of Arnórsson -2000

Quartz geothermometer of Verma -2000

Equation

$\{777/[\log(\text{Na}/\text{K}) + 0.700]\}-273.15$
$\{855.6/[\log(\text{Na}/\text{K}) + 0.8573]\}-273.15$
$\{1,217(\pm 93.9)/[\log(\text{Na}/\text{K}) + 1.483]\}-273.15$
$\{833/[\log(\text{Na}/\text{K}) + 0.780]\}-273.15$
$\{933/[\log(\text{Na}/\text{K}) + 0.993]\}-273.15$
$\{1,319/[\log(\text{Na}/\text{K}) + 1.699]\}-273.15$
$\{1,178/[\log(\text{Na}_m/\text{K}_m) + 1.239]\}-273.15$
$\{1,390/[\log(\text{Na}/\text{K}) + 1.75]\} 273.15$
$\{1,289(\pm 76/[\log(\text{Na}/\text{K}) + 0.615])\}-273.15$
$733.6-770.551[\log(\text{Na}_m/\text{K}_m)] + 378.189[\log(\text{Na}_m/\text{K}_m)]^2-95.753[\log(\text{Na}_m/\text{K}_m)]^3 + 9.544[\log(\text{Na}_m/\text{K}_m)]^2$
$\{1,052/[1-\exp(1.714(\log(\text{Na}/\text{K}) + 0.252))]\} + 76$
$\{883(\pm 15)/[\log(\text{Na}/\text{K}) + 0.894(\pm 0.032)]\}-273.15$
$\{833/[\log(\text{Na}/\text{K}) + 0.908]\}-273.15$
$\{4,410/[14.0-\log(\text{K}^2/\text{Mg})]\}-273.15$
$\{2,200/[5.47-\log(\text{Li}/(\text{Mg}^{0.5}))]\}-273.15$
$\{1,910/[4.63-\log(\text{Li}/(\text{Mg}^{0.5}))]\}-273.15$
$\{1,000(\pm 47)/[\log(\text{Na}_m/\text{Li}_m) + 0.38(\pm 0.11)]\}-273.15$
$\{1,195(\pm 75)/[\text{Log}(\text{Na}_m/\text{Li}_m)-0.19(\pm 0.25)]\}-273.15$
$\{1,590/[\log(\text{Na}/\text{Li}) + 0.779]\}-273.15$
$\{1,049(\pm 44)/[\log(\text{Na}_m/\text{Li}_m) + 0.44(\pm 0.10)]\}-273.15$
$\{1,267(\pm 35)/[\log(\text{Na}_m/\text{Li}_m) + 0.07(\pm 0.10)]\}-273.15$
$\{11,140/[6 \log(\text{Na}_m/\text{K}_m) + \log(\text{Mg}_m/(\text{Na}_m)^2) + 18.30]\}-273.15$
$[1,309/(5.19-\log S)]-273.15$
$[1,522/(5.75-\log S)]-273.15$
$\pm 1.345) + 0.28831(\pm 0.01337)S - 3.6686 \times 10^{-4} (\pm 3.152 \times 10^{-5})S^2 + 3.1665 \times 10^{-7} (\pm 2.421 \times 10^{-7})S^3 + 77.034(\pm 1.0$
$-\{44.119(\pm 0.438)\} + \{0.24469(\pm 0.00573)\}S - \{1.7414 \times 10^{-4} (\pm 1.365 \times 10^{-5})\}S^2 + \{79.305(\pm 0.427)\} \log S$
$-55.3 + 0.3659S - 5.3954 \times 10^{-4} S^2 + 5.5132 \times 10^{-7} S^3 + 74.360 \log S$
$\{[1,175.7(\pm 31.7)]/[4.88(\pm 0.08)-\log S]\}-273.15$

$216) \log S$
